Title: **Unidirectional trans-Atlantic gene flow and a mixed spawning area shape the genetic connectivity of Atlantic bluefin tuna**

Running title*:* **Genetic connectivity of Atlantic bluefin tuna**

Natalia Díaz-Arce[1*], Pierre-Alexandre Gagnaire[2], David E. Richardson[3], John F. Walter III[4], Sophie Arnaud-Haond[5], Jean-Marc Fromentin[5], Deirdre Brophy[6], Molly Lutcavage[7], Piero Addis[8], Francisco Alemany[9], Robert Allman[10], Simeon Deguara[11], Igaratza Fraile[12], Nicolas Goñi[12#], Alex R Hanke[13], F Saadet Karakulak[14], Ashley Pacicco[15], Joseph M Quattro[16], Jay R Rooker[17], Haritz Arrizabalaga[12] and Naiara Rodríguez-Ezpeleta[1,*]

*Correspondence: ndiaz@azti.es; nrodriguez@azti.es;

[1] AZTI Marine Research, Basque Research and Technology Alliance (BRTA), Sukarrieta, Spain

[2] ISEM, Univ Montpellier, CNRS, EPHE, IRD, Montpellier, France

[3] Northeast Fisheries Science Center, National Marine Fisheries Service, National Oceanic and Atmospheric Administration (NOAA), Narragansett, RI, USA

[4] Southeast Fisheries Sciences Center, National Marine Fisheries Service, National Oceanic and Atmospheric Administration (NOAA), Miami, FL, USA

[5] MARBEC, Univ Montpellier, Ifremer, IRD, CNRS, Sète, France

[6] Marine and Freshwater Research Center, Atlantic Technological University (ATU), Galway City, Ireland

[7] Large Pelagics Research Center, School for the Environment, University of Massachusetts Boston, Gloucester, MA, USA

[8] Department of Environmental and Life Science, University of Cagliari, Cagliari, Italy

[9] International Commission for the Conservation of Atlantic Tunas, GBYP, Madrid, Spain

[10] National Marine Fisheries Service, Southeast Fisheries Science Center, Panama City Laboratory, Panama City, FL, USA.

[11] AquaBio Tech Ltd., Central Complex, Mosta, Malta

[12] AZTI Marine Research, Basque Research and Technology Alliance (BRTA), Pasaia, Spain

[13] St Andrews Biological Station, Fisheries and Oceans Canada, St. Andrews, New Brunswick, Canada

[14] Faculty of Aquatic Sciences, Istanbul University, Istanbul, Turkey

[15] Cooperative Institute for Marine and Atmospheric Studies Rosenstiel School of Marine, Atmospheric and Earth Science, University of Miami, Miami, FL, USA

[16] Department of Biological Sciences, University of South Carolina, Columbia, SC, USA

[17] Department of Marine Biology, Texas A&M University at Galveston, Galveston, TX, USA

[#] Present address: Fisheries and Fish Resources, Natural Resources Institute Finland, Turku, Finland

Abstract *[<250 words]*

The commercially important Atlantic bluefin tuna (*Thunnus thynnus*), a large migratory fish, has experienced notable recovery aided by accurate resource assessment and effective fisheries management efforts. Traditionally, this species has been perceived as consisting of eastern and western populations, spawning respectively in the Mediterranean Sea and the Gulf of Mexico, with mixing occurring throughout the Atlantic. However, recent studies have challenged this assumption by revealing weak genetic differentiation and identifying a previously unknown spawning ground in the Slope Sea used by Atlantic bluefin tuna of uncertain origin. To further understand the current and past population structure and connectivity of Atlantic bluefin tuna, we have assembled a unique dataset including thousands of genome-wide single nucleotide polymorphisms (SNPs) from 500 larvae, young of the year and spawning adult samples covering the three spawning grounds and including individuals of other *Thunnus* species. Our analyses support two weakly differentiated but demographically connected ancestral populations that interbreed in the Slope Sea. Moreover, we also identified signatures of introgression from albacore (*Thunnus alalunga*) into the Atlantic bluefin tuna genome, exhibiting varied frequencies across spawning areas, indicating strong gene flow from the Mediterranean Sea towards the Slope Sea. We hypothesize that the observed genetic differentiation may be attributed to increased gene flow caused by a recent intensification of westward migration by the eastern population, which could have implications for the genetic diversity and conservation of western populations. Future conservation efforts should consider these findings to address potential genetic homogenization in the species.

Keywords [4-6]:

atlantic bluefin tuna, genetic connectivity, introgression, large migratory fish, single-nucleotide polymorphisms

Introduction

Conservation of fisheries resources relies on the assessment and management of self-sustaining units called stocks, whose delimitation often oversimplifies species population dynamics (Begg et al., 1999, Stephenson, 1999, Reiss et al., 2009). Yet, failing to account for stock complexity can induce overfishing and ultimately result in fisheries collapse (Hutchinson, 2008), highlighting the importance of integrating knowledge on spatial structure and connectivity into management plan development processes (Kerr et al., 2016). In this context, the potential of genomic approaches is increasingly being harnessed to tackle a diverse range of fisheries management related questions. Among these are assessment of population structure, connectivity and adaptation to local environments (Bernatchez et al., 2017; Ovenden et al., 2015), even when genetic differentiation is low, as observed in highly migratory fish like striped marlin (Mamoozadeh et al., 2020), blue shark (Nikolic et al., 2023) and yellowfin tuna (Barth, Damerau, et al., 2017). While the study of neutral (not affecting individuals fitness) and adaptive (those that affect individuals fitness) variants separately can provide with complementary information relevant for fisheries science (Mariani & Bekkevold, 2014), the preservation of fish genetic diversity and conservation of locally adapted populations has gained importance in the face of rapid environmental changes and increasing fishing pressure (Bonanomi et al., 2015). Species resilience may depend on their adaptive capacities (Bernatchez, 2016; Hoffmann & Sgrò, 2011), making the inclusion of adaptive variation in genomic studies focusing on managed fisheries target species essential (Fraser & Bernatchez, 2001; Valenzuela-Quiñonez, 2016; Xuereb et al., 2021).

The Atlantic bluefin tuna (ABFT, *Thunnus thynnus*) is a large and emblematic highly migratory species that inhabits waters of the North Atlantic Ocean and adjacent seas (Collette et al., 2011; Fromentin & Powers, 2005). ABFT has been heavily exploited for millennia and the emergence of the sushi-sashimi market in the 1980s turned it into one of the most valuable tuna species in the international fish trade (Fromentin, Bonhommeau, et al., 2014). This high value, coupled with poor governance, led to three decades of high fishing pressure and ultimately to overexploitation. Following the implementation of a strict management plan in the late 1990s, signs of population rebuilding have been documented (ICCAT, 2021). However by 2011, ABFT was considered endangered by the IUCN (Collette et al., 2011). Uncertainties around ABFT biology suggest that an overly simplistic management paradigm could compromise the long-term conservation of the species (Brophy et al., 2020; Fromentin, Bonhommeau, et al., 2014). ABFT has been managed as two separate units since 1981: the western and eastern stocks, which are separated by the 45°W meridian and are assumed to originate from the two spawning areas located in the Gulf of Mexico and the Mediterranean Sea respectively (ICCAT, 2019). Several studies on the population structure and stock dynamics support two reproductively isolated spawning components (Gulf of Mexico and the Mediterranean Sea): electronic tagging studies (Block et al., 2005) have found no individual visiting both spawning areas, and otolith chemical signatures (Rooker et al., 2014) and genetic data (Rodríguez-Ezpeleta et al., 2019) support spawning-site fidelity. Nevertheless, numerous studies also detected evidence of regular trans-Atlantic movements across the 45°W meridian boundary line and of mixed foraging grounds along the North Atlantic (Arregui et al., 2018; Block et al., 2005; Rodríguez-Ezpeleta et al., 2019; Rooker et al., 2014). In response to these findings, the International

Commission for the Conservation of Atlantic Tunas (ICCAT) recently adopted a management procedure for ABFT that accounts for mixing between the two stocks (ICCAT, 2023). Given recent advancements in stock of origin assignment and increased samples from the mixing areas, it is important to determine if the modelled dynamics are consistent with the new data on mixing proportions. Specifically, when applying individual origin assignment based on subsets of informative genetic markers of ABFT captured in the North Atlantic Ocean (Puncher et al., 2022; Rodríguez-Ezpeleta et al., 2019), it was observed that 10%-25% of individuals could not be clearly assigned to either spawning ground. Moreover, a combined analysis of genetic and otolith microchemistry data resulted in contrasting or unresolved origin assignments (Brophy et al., 2020).

Amidst uncertainty surrounding ABFT stock dynamics, the recent discovery of ABFT larvae in the Slope Sea, located between the Gulf Stream and the northeast Unite States continental shelf (Richardson et al., 2016a), adds another layer of complexity to our knowledge of the reproductive ecology of the species. Subsequent oceanographic studies (Rypina et al., 2019) and larval collections (Hernández et al., 2022) provide additional evidence of spawning activity in this area. Tagging information further revealed that mature size fish occurred in the Slope Sea in spring and summer coinciding with the spawning season estimated for the found larvae (Galuardi et al., 2010), and age-structure spawning in the western Atlantic has been hypothesized based on tagging, longline catch data and reproductive studies data, meaning that younger fish would preferably spawn in the Slope Sea and only bigger fish would spawn in the Gulf of Mexico (Richardson et al., 2016a). The implications of Slope Sea spawning generated debate and controversy (Richardson et al., 2016b; Safina, 2016; Walter et al., 2016), with one of the

key unknowns being the connectivity between the Slope Sea and the other two spawning grounds. In addition, some studies found evidence of migratory changes in ABFT, including the re-colonization (Aarestrup et al., 2022; Horton et al., 2020; Nøttestad et al., 2020) and even expansion (Jansen et al., 2021) of its geographic range. These changes coincided with a strong recovery of the Mediterranean Sea spawning biomass during the last two decades and the increased presence of eastern origin fish in the western Atlantic (Aalto et al., 2021).

To disentangle the population structure and connectivity of ABFT, we genotyped and analysed thousands of genome-wide single-nucleotide polymorphism (SNPs) from a total of approximate 500 ABFT larvae, young of the year and adults from the two well-known spawning grounds (Gulf of Mexico and Mediterranean Sea) as well as the recently discovered Slope Sea spawning ground. We studied individual genomic diversity, tested for admixture between spawning grounds and inferred the demographic history of ABFT for the first time. Mitochondrial introgression from albacore *(Thunnus alalunga*) into ABFT has been previously reported, with all introgressed individuals detected so far found in the Mediterranean Sea and the Slope Sea (Alvarado Bremer et al., 2005; Viñas et al., 2011), but not in the Gulf of Mexico. We screened for adaptive genomic variation, incorporating samples from other *Thunnus* species to evaluate the impact of gene flow between species as an additional contribution to adaptive genomic diversity. Finally, we integrated information obtained from neutral, potentially adaptive and introgressed genetic markers to reconstruct the connectivity patterns of the ABFT across its entire distribution.

Methods

166 A summarized schematic view of samples and methods is shown in Figure S1.

167

168 *Sampling, DNA extraction and additional data collection*

169 Larvae, young of the year (individuals less than 3 kg weight) and adult (more than 100
170 kg weight individuals) samples of ABFT from the Mediterranean Sea (*n*=260), the Gulf of
171 Mexico (*n*=210) and the Slope Sea (*n*=49) were obtained from scientific surveys and
172 commercial fisheries from these three spawning grounds (Table S1; Figure 1a). From
173 each adult and young of the year, a ~1 cm^3 piece of muscle or fin tissue sample was
174 excised and immediately stored in RNA-later or 96% molecular grade ethanol at -20°C
175 until DNA extraction. Larvae were collected with a 60 cm diameter bongo net or a 2 x 1
176 m frame net and immediately preserved in 96% molecular grade ethanol. Genomic DNA
177 was extracted from about 20 mg of tissue or from whole (only if larvae were of less than
178 8mm, which corresponds with the category of preflexion or intermediate and therefore
179 these are not expected to have predated over other larvae of their same species which
180 could be confounded with sample contamination) or partial larvae (eyeballs or tails)
181 using the Wizard® Genomic DNA Purification kit (Promega), following manufacturer's
182 instructions for 'Isolating Genomic DNA from Tissue Culture Cells and Animal Tissue'.
183 Extracted DNA was suspended in Milli-Q water and concentration was determined with
184 the Quant-iT dsDNA HS assay kit using a Qubit® 2.0 Fluorometer (Life Technologies).
185 DNA integrity was assessed by electrophoresis, migrating about 100 ng of GelRed™-
186 stained DNA on a 1.0% agarose gel. For selected specimens, spawning capability was
187 assessed by histologic inspection following the criteria described in Brown-Peterson et
188 al. (2011). Additionally, for females, ovulation within the past 2 days was determined
189 from identification of post-ovulatory follicle complexes, which are assumed to degrade

within 24-48 h (Aranda et al., 2011; McPherson, 1991; Schaefer, 1996). For selected adult specimens, sagittal otoliths were prepared for analysis of stable isotope signatures of the otolith core (yearling period) according to the protocol described in Rooker et al. (2008) and analysed for $\delta^{13}C$ and $\delta^{18}O$ on an automated carbonate preparation device (KIEL-III, Thermo Fisher Scientific, Inc.) coupled to a gas-ratio mass spectrometer (Finnigan MAT 252, Thermo Fisher Scientific, Inc.) at the University of Arizona. Stable isotopes of carbon and oxygen ($\delta^{13}C$ and $\delta^{18}O$) are reported relative to the PeeDee Belemnite (PDB) scale after comparison to an in-house laboratory standard calibrated to PDB.

Cytochrome oxidase subunit I gene fragment amplification and sequencing and diagnostic variant identification

A fragment of the mitochondrial cytochrome oxidase subunit I (COI) gene was amplified for a representative subset of 86 individuals using the FishF1 (5'-244 TCAACCAACCACAAAGACATTGGCAC-3') and FishR1 (5'-TAGACTTCTGGGTGGCCAAAGAATCA-3') primers (Ward et al., 2005) in a total volume of 20 µL with 0.2 µL of Dream Taq Polymerase (Thermo Fisher Scientific), 2 µL of Dream Taq Buffer 10X (Thermo Fisher Scientific), 0.4 µL of each primer and 50 ng of total DNA using the following profile: an initial denaturation step at 95°C for 3 min, 35 cycles of 30 s at 98°C, 30 s at 54°C and 60 s at 72°C, and a final extension of 72°C for 10 min. Products were visualized on 1.7% agarose gels, purified with GE Healthcare Illustra ExoProStar™ (ref. US77705) and Sanger sequenced. The newly generated 86 sequences were edited using SeqTrace 0.9.0, submitted to GenBank (accession nos MT037084-MT037149, MT037151-MT037170) and aligned with BioEdit (v7.2.5) together with other publicly

available representative COI sequences of albacore tuna (*T. alalunga*; accession no. KT074102) and ABFT (accession no. DQ107585), including the alalunga-like (accession no. GQ414567) haplotypes (Table S2). Diagnostic positions between ABFT and albacore haplotypes were used to detect mitochondrial introgression from albacore to ABFT samples.

RAD-seq library preparation, sequencing and read filtering

Restriction-site-associated DNA libraries of 519 ABFT individuals were prepared following Etter et al. (2012). Input DNA (ranging from 50 to 500 ng) was digested with the *SbfI* restriction enzyme and ligated to modified Illumina P1 adapters containing 5 bp unique barcodes. Pooled DNA of 32 individuals was sheared using the Covaris® M220 focused-ultrasonicator™ instrument (Life Technologies) and size selected to 300-500 bp on agarose gel. After Illumina P2 adaptor ligation, each library was amplified using 14 PCR cycles. Each pool was paired end sequenced (100 bp) on an Illumina HiSeq2000. De-multiplexing, quality filtering (removing reads with an average Phred score is lower than 20 and truncating them to 90 nucleotides to remove low-quality bases at the sequence end) and PCR duplicate removal were performed using the *process_radtags* and *clone_filter* modules of *Stacks* version 2.3e (Rochette et al., 2019).

RAD-tag assembly and SNP calling

Five RAD-seq derived catalogues (Figure S1; Table S3) were generated. Three of them included ABFT individuals and were either de novo assembled ('nuclear de novo') or mapped to the Pacific bluefin tuna nuclear (PBFT, *Thunnus orientalis*) (Suda et al., 2019) or ABFT mitochondrial (accession no. NC_014052) genomes ('nuclear mapped' and

238 'mito'). The other two catalogues were mapped to the PBFT genome and included all
239 ABFT individuals and four Southern bluefin tuna (*Thunnus maccoyii*), four albacore and
240 five PBFT individuals (Díaz-Arce et al., 2016) ('nuclear mapped + others') or only ABFT
241 larvae and four albacore individuals ('nuclear mapped + ALB'). Both reference-mapped
242 and de novo-assembled catalogues were generated for testing possible bias introduced
243 by the use of the reference genome from a closely related species, which is less
244 fragmented than the one available for ABFT (accession no. GCA_003231725). The three
245 nuclear-mapped catalogues were generated including different sets of individuals as
246 described earlier to maximize the number of informative markers included for each type
247 of analysis. In order to avoid inclusion of kins in the resulting datasets, which could bias
248 some population structure results, a genetic relatedness matrix using the GCTA toolbox
249 (Yang et al., 2011) was generated using the genotypes obtained from the 'nuclear
250 mapped' catalogue (generated as described next), and only one individual (the one with
251 the highest number of assembled RAD tags) of each resulting pair with relatedness
252 higher than 0.1 (threshold selected after visual inspection of the distribution of the
253 genetic relatedness values) was included in subsequent analyses. Reference-based
254 assemblies were performed by mapping the quality-filtered reads to the corresponding
255 reference genome using the BWA-MEM algorithm (Li, 2013) using default mapping
256 parameters, converting the resulting SAM files to sorted and indexed BAM files using
257 SAMTOOLS (Li et al., 2009) and filtering the mapped reads to include only primary
258 alignments and correctly mate mapped reads. De novo assembly was performed using
259 the *ustacks, cstacks, sstacks* and *tsv2bam* modules of Stacks version 2.3e with a
260 minimum coverage depth of three reads per allele (i.e. each of the two possible versions
261 of one bi-allelic SNP variant), a maximum of two nucleotide mismatches between two

alleles at a same locus and a maximum of six mismatches between loci (Rodríguez-Ezpeleta et al., 2019). For all mapped and de novo catalogues, SNPs were called using information from paired end reads with the *gstacks* module of Stacks version 2.3e. For the 'mito' catalogue, only samples with no missing data for the three diagnostic positions used for detecting introgression were kept, and the heterozygous genotypes, considered to be related to sequencing or assembly errors, were removed. For the rest of the RAD catalogues, only samples with more than 25,000 RAD loci and SNPs contained in RAD loci present in at least 75% of the ABFT ('nuclear mapped' and 'de novo') or in 75% of the individuals from each of the species included ('nuclear mapped + others' and 'nuclear mapped + ALB') were kept and exported into PLINK (Purcell et al., 2007) using the *populations* module of *Stacks* version 2.3e. Using only SNPs derived from read 1, increasing threshold values for minimum genotyping rate for individuals and SNPs were applied to obtain a final genotype table with a minimum genotyping rate of 0.95 and 0.85 per SNP and individual respectively (except for the 'nuclear mapped + ALB' catalogue for which thresholds were 0.95 and 0.90 respectively). SNPs were filtered using different minor allele frequency (MAF) thresholds considering sample sizes of the different datasets to exclude from the analysis rare non-informative variants that are susceptible to being derived from sequencing or assembly errors. For the 'nuclear mapped' and 'nuclear de novo' catalogues, SNPs with a MAF < 0.05 were removed, for the 'nuclear mapped + others' catalogue, SNPs with MAF < 0.05 in ABFT and MAF <0.25 in each of the other species were removed, and for the 'nuclear mapped + ALB' catalogue, SNPs with a minimum allele count of two in ABFT and those variable within albacore were removed. For all nuclear catalogues, SNPs failing Hardy Weinberg equilibrium test at a p-value threshold of .05 in Mediterranean Sea larvae or Gulf of

Mexico larvae groups were removed. Resulting genotype tables including all SNPs or only the first SNP per tag were converted to Genepop, Structure, PLINK, BayeScan, immanc, VCF and TreeMix formats using *populations* or PGDSpider version 2.0.8.3 (Lischer & Excoffier, 2011). From the 'mito' catalogue, genotypes for three diagnostic positions used for detecting introgression identified though comparison of COI sequences (see *Cytochrome oxidase subunit I gene fragment amplification and sequencing and diagnostic variant identification* subsection earlier) were extracted using PLINK (Purcell et al., 2007).

Genetic diversity and population structure estimates

The following analyses were performed on the 'nuclear mapped' and 'nuclear de novo' datasets including only the first SNP per tag. Genome-wide average and per-SNP pairwise F_{ST} values were calculated using Genepop (Raymond, 1995) both including all individuals or only larvae. Significance ($p<.05$) of F_{ST} values was estimated by performing 10,000 permutations. Principal component analysis (PCA) was then performed using the adegenet R package (Jombart & Ahmed, 2011) to illustrate the main axes of genetic variation among individuals. The number and nature of distinct genetic clusters was investigated using the model based clustering method implemented in ADMIXTURE (Alexander et al., 2009) assuming from 2 to 5 ancestral populations (K) and setting 5000 bootstrap runs. A first ADMIXTURE run was launched for each value of K to check the number of steps necessary to reach the default 0.001 likelihood value during the first run. This information was used to set the '-c' parameter (steps to be fulfilled in each bootstrapped run) that would assure convergence for each analysis (from 20 to 100 steps) for the bootstrapped runs. The value of K (ranging from 2 to 10) with lowest

310 associated error value was identified using ADMIXTURE's cross-validation procedure.
311 The convert function from ADMIXTOOLS software (Patterson et al., 2012) was used to
312 convert from PLINK to eigenstrat format and the qp3Pop function was used to calculate
313 F3 statistic and Z-score associated values (Patterson et al., 2012), testing for all possible
314 admixture scenarios grouping separately samples from different locations and age
315 classes (Table S4) on the 'nuclear-mapped' catalogue dataset.
316
317 *Demographic history*
318 We used the unfolded three-dimensional joint Site Frequency Spectrum (3D-JSFS) to
319 infer the ABFT demographic history. The 3D-JSFS was constructed for Mediterranean
320 Sea, Slope Sea and Gulf of Mexico populations using the allele counts of bi-allelic variants
321 included in the VCF file obtained from the 'nuclear mapped + ALB' catalogue, which
322 included four albacore samples for variant orientation. Derived allele counts were
323 averaged over all possible re-sampling of 20 genotypes within each of the three ABFT
324 locations and singletons were excluded using a minimum allele count filter of two. We
325 performed historical demographic model comparison by fitting separately 10 candidate
326 models (Table S5) to the observed JSFS using a diffusion approximation approach
327 implemented in δaδi v1.7.0 (Gutenkunst et al., 2009) and an optimization routine based
328 on consecutive rounds of optimizations (Portik et al., 2017). We adapted existing
329 divergence models to include the three different possible dichotomous branching of the
330 three populations involving two splits, a simultaneous split of the three populations
331 from an ancestral populations and a scenario of split between the Mediterranean Sea
332 and Gulf of Mexico populations followed by an admixed origin of the Slope Sea. We
333 fitted each of these divergence scenarios with or without allowing constant migration

rates between populations from split to present. Ancestral effective population size (N_A), migration rates and time estimates scaled to theta ($4N_A\mu$) and the percentage of variable sites correctly oriented with respect to the ancestral state were estimated for all models. Model selection was performed using the Akaike information criterion and goodness of fit was assessed by generating 100 Poisson-simulated SFS from the model SFS, fitting the model to each simulated SFS and using the log-likelihood and log-transformed chi-squared test statistic to generate a distribution of simulated data values against which the empirical values can be compared (Portik et al., 2017).

Loci under selection

Loci potentially influenced by selection were screened from the 'nuclear mapped' catalogue considering all SNPs using two approaches. The reversible jump Markov chain Monte Carlo approach implemented in BAYESCAN 2.1 (Foll & Gaggiotti 2008) was applied by grouping samples per location, setting default parameters of 50,000 burn-in steps, 5000 iterations, 10 thinning interval size and 20 pilot runs of size 5000. Candidate loci under selection with a posterior probability higher than 0.76 (considered as strong according to the Jeffery's interpretation in the software manual) and a false discovery rate (FDR) lower than 0.05 were selected. We then used the multivariate analysis method implemented in the pcadapt R package, which does not require a prior grouping of the samples, following Luu et al. (2017) recommendations and selected outlier SNPs following the Benjamini-Hochberg procedure. Sequences of the RAD loci containing outlier SNPs were obtained using the *populations* module of *Stacks* version 2.3e and mapped against the annotated reference genome of *Thunnus albacares* (accession no. GCA_914725855) using the BWA-MEM algorithm (Li, 2013) using default mapping

parameters. Pairwise linkage disequilibrium between all filtered SNPs obtained from those scaffolds which contained candidate SNPs under selection was measured using the R package LDheatmap. PCAs were performed using the adegenet R package (Jombart & Ahmed 2011) based on outlier SNPs, and variants obtained from one genomic region found to be under high linkage disequilibrium from the 'nuclear mapped' and the 'nuclear mapped + others' catalogues. Individual heterozygosity values based on SNPs within and out from this region from the 'nuclear mapped', and test for Hardy Weinberg equilibrium of identified haplotype groups were calculated using PLINK (Purcell et al., 2007).

Tests for nuclear introgression

Nuclear introgression from albacore to ABFT was tested by applying the statistical model implemented in TreeMix (Pickrell & Pritchard, 2012) and ABBA/BABA analyses (Durand et al., 2011; Green et al., 2010; Kulathinal et al. 2009) on 'nuclear mapped + other' dataset with only one SNP per tag to avoid including variants in high linkage. The latter test was also performed excluding or including only those SNPs located within the genomic region found under high linkage disequilibrium [scaffolds BKCK01000075 (partially) and BKCK01000111]. TreeMix was used to estimate historical relationships among populations and species by estimating the maximum likelihood tree for a set of populations allowing historical gene flow events. TreeMix was run allowing from 0 to 10 migration events, obtaining an increasing number of possible gene flow events and associated likelihood values. We followed the author's recommendations (Pickrell & Pritchard, 2012) to select the most probable number of migration events by stopping adding additional migration events as long as the results remained interpretable and

selecting the number showing best-associated likelihood value. The ABBA/BABA test, which measures the excess of derived alleles shared between a candidate donor species and one of two tested groups (in this case, one ABFT group) compared with the other group taken as a reference (a different ABFT group), was performed on the allele frequencies of the derived allele in albacore and ABFT locations, based on the ancestral state defined by the Southern bluefin tuna taken as an out-group. Derived alleles frequencies were estimated using a python script available at https://github.com/simonhmartin/genomics_general. Patterson's D statistic was calculated using R for all possible combinations of target and reference groups of ABFT, always considering albacore as the candidate donor species. Additionally, inter-species absolute divergence (dxy) between Mediterranean ABFT larvae and albacore individuals was estimated at each polymorphic position from the 'nuclear mapped + other' catalogue. PCAs were performed using the adegenet R package (Jombart & Ahmed, 2011) based on all filtered SNPs and only those SNPs from the region under high linkage disequilibrium from the 'nuclear mapped + others' catalogue.

Results

Genetic differentiation between Atlantic bluefin tuna spawning components

We studied the population genetic structure and connectivity of ABFT using a genome-wide SNP dataset. Our study includes reference samples (*i.e.,* larvae and young of the year ABFT captured at or close to where they were hatched and adults caught on the spawning grounds during the spawning season) from the Gulf of Mexico and Mediterranean Sea, and from a more recently discovered spawning ground in the Slope

406 Sea used by ABFT of unknown origin (Figure 1a, Table S1). Consistent genetic
407 differentiation between samples from these three spawning grounds was revealed by
408 both an unsupervised clustering analysis of genetic ancestry (ADMIXTURE) (Figures 1b
409 and S2a) and a PCA (Figure 1c and S2b), with significant pairwise genetic differentiation
410 (F_{ST}) between reference larvae from different spawning grounds ranging from 0.0007
411 (Slope Sea – Gulf of Mexico) to 0.003 (Mediterranean Sea – Gulf of Mexico) (Table S6).No
412 fixed nor private alleles were found between spawning areas. This contemporary
413 genetic structure was associated with a mixture of two genetic ancestries (Figure S3),
414 hereafter called GOM-like, predominant in the Gulf of Mexico (average GOM-like
415 ancestry proportion across Gulf of Mexico individuals was 0.81 SD ± 0.22), and MED-like,
416 predominant in the Mediterranean Sea (average MED-like ancestry proportion across
417 Mediterranean individuals was 0.82 SD ± 0.11). Additionally, whereas all Mediterranean
418 individuals had a homogeneous MED-like genetic origin, ancestry profiles of Gulf of
419 Mexico individuals were more variable, including 15 adults (out of 156) (Table S1) with
420 a clear MED-like genetic profile (average GOM-like proportion across Gulf of Mexico
421 individuals excluding 15 MED-like was 0.86 SD ± 0.14) (Figure 1c,d). Otolith
422 microchemistry composition available for 6 of these 15 MED-like adults is compatible
423 with Mediterranean Sea origin (Figure S4) and gonad histology inspection confirmed
424 that 14 of them were spawning capable, including one female that had ovulated less
425 than 48 h prior to capture (Table S1). Compared to the Gulf of Mexico and the
426 Mediterranean Sea, the Slope Sea showed a large variance in individual ancestries
427 ranging from GOM-like to MED-like, with a high proportion of admixed ancestries
428 (average GOM-like proportion across Slope Sea individuals was 0.68 SD ± 0.22) (Figure
429 1d). In agreement with these results, admixture tests (F3 statistics) showed that the

Slope Sea component is the result of admixture between the two other components (Figure 1e, S5 and Table S4). No admixture was found in the Mediterranean Sea, nor in larvae from the Gulf of Mexico. In contrast, admixture was detected in adult samples from the Gulf of Mexico (Figure 1e). Demographic history inferences (∂a∂i) supported that the Slope Sea and the Gulf of Mexico spawning components share a recent common ancestry, and that there is strong contemporary migration from the Mediterranean Sea and the Gulf of Mexico towards the Slope Sea (Figures 1f, S6 and Table S5). Migration rates in all other directions are much weaker, the strongest being the migration from the Slope Sea back to the Gulf of Mexico, which is three times lower than in the opposite direction.

Observed genetic differentiation between Atlantic bluefin tuna spawning components cannot be attributed to local adaptation acting on few loci of large effect

To better understand the evolutionary processes behind genetic differentiation in ABFT, we separately studied genetic diversity at neutral (i.e. those that are mostly influenced by genetic drift and migration) and outlier SNPs markers (i.e. those that are potentially under selection or in tight linkage with selected loci). Removing the 123 identified outlier markers did not change the overall population structure pattern nor differentiation values (Figure S7), suggesting that observed genetic differentiation cannot be explained by local adaptation only. On the other hand, analyses based on the 123 markers identified as potentially under selection provided higher genetic differentiation values among spawning grounds (Figure S8), but revealed three groups of samples that do not correspond to the overall population structure (Figures 2a and S8) and that are neither

454 related to laboratory nor phenotypic sex effects (Figure S9). These 123 outliers were
455 located within 104 different assembled RAD tags, whose sequences mapped against the
456 annotated reference genome of *T. albacares*, among which 84 were located within
457 protein coding genes (Table S7). The 20% of the SNP markers that contribute the most
458 to this grouping are located within the same region of the genome (mapping on two
459 scaffolds spanning 2.63 Mb region of the PBFT reference genome) (Table S8) and show
460 strong pairwise linkage disequilibrium (LD) across the whole region (meaning that
461 variant versions of SNP pairs are non-randomly associated and the same combination is
462 often found among individuals haplotypes) (Figure 2b). The SNPs located within this
463 high-LD region, which mapped to the same chromosome of the *T. albacares* reference
464 genome (Table S7), support a three-grouping pattern (Figure S10a), with the
465 intermediate group of individuals in the PCA presenting increased heterozygosity values
466 (Figures 2c, S10b). This suggests the existence of two main haplotypes (unique allelic
467 combinations across multiple SNPs) in this region combined into three possible
468 genotypes (e.g. AA, AB, BB), which shows characteristics typical of a chromosomal
469 inversion. These two haplotypes, presumably the inverted and collinear versions, are
470 present at different frequencies among spawning grounds, the rarest found to be
471 homozygous only in the Mediterranean Sea, where it is more frequent, and the
472 alternative being more abundant in the Gulf of Mexico and Slope Sea (Figure 2d). The
473 variants of this inversion, if considered as one single marker, were under Hardy-
474 Weinberg equilibrium ($p < 0.05$) within each group showed in Figure 2d.
475
476 *Gene flow from Mediterranean Sea towards the Slope Sea revealed by inter-specific*
477 *introgression*

To understand why genetic differentiation is maintained despite presumable ongoing gene flow, we studied the potential adaptive effect of inter-specific introgression. According to three diagnostic positions for mitochondrial ancestry (Table S2), we found albacore origin introgressed mitochondria in individuals of all age classes not only in both the Mediterranean Sea (4%) and the Slope Sea (6%), but also to a lower extent in Gulf of Mexico adults (1%) (Figure 3a and Table S1). These results were confirmed at the nuclear level by a tree-based analysis of population splits and admixture using allele frequency data (TreeMix), which supported an introgression event from albacore into the Mediterranean Sea ABFT (Figure 3a and S11). In accordance with this deviation from a strict bifurcating evolutionary history, we also found an excess of derived allele sharing between albacore and both the Slope Sea and the Mediterranean Sea with respect to the Gulf of Mexico (ABBA/BABA test, Figure 3b). To test if the genetic differentiation between Mediterranean Sea and Gulf of Mexico ABFT populations was driven by introgressed alleles of albacore origin we estimated genetic diversity between the Mediterranean ABFT and albacore individuals at each SNP, which were positively correlated with F_{ST} values between Mediterranean Sea and Gulf of Mexico ABFT (Figure S12).

A PCA based on genetic markers from the genomic region which contained most outlier SNPs and including other *Thunnus* species (Figure 4a) showed that homozygous individuals for the most abundant haplotype group associated with the PBFT, whereas those homozygous for the rarest variant were closer to albacore. By contrast, the PCA based on the genome-wide SNP dataset showed the expected grouping pattern reflecting species membership, where PBFT and ABFT cluster together and were separated from albacore and Southern bluefin tunas (Figure S13). Test for deviation

from a strict bifurcating evolutionary history (ABBA/BABA) showed a much more pronounced signal of introgression from albacore into the Mediterranean and Slope Sea spawning ground samples in the high-LD region showing nearly 10 times higher D-statistic values (Figure 4b) than when considering the overall genome (Figure 3b). Yet, this pattern remained when removing all SNPs from the high-LD region (Figure S14), indicating that the signal of introgression is present genome-wide.

These results suggest that the genetic differentiation observed between ABFT from different spawning grounds is maintained despite gene flow between the Mediterranean Sea and the Slope Sea and cannot be explained by local adaptation acting on a few loci of large effect. Additionally, a large genomic region of albacore ancestry, introgressed into the ABFT genome in the Mediterranean Sea, has retained high LD while expanding towards the western Atlantic, following the previously detected genome-wide signal of albacore ancestry. Altogether, our results point towards a situation where the two ancestral genetic components of ABFT (western Atlantic and Mediterranean) have initially diverged in isolation, independently experiencing genetic drift combined with introgression of genetic material from albacore in the Mediterranean Sea. More recently, homogenization between western Atlantic and Mediterranean components could have been initiated by the intensification of gene flow, without completely eroding existing genetic differentiation.

Discussion

525 Understanding demographic patterns in migratory fish species with complex
526 evolutionary histories requires the integration of various data sources, ranging from
527 genetic markers, which can be affected by different evolutionary forces and reveal
528 reproductive isolation or local adaptation, to otolith microchemistry signals, which
529 reveal life span spatial distributions. However, such integrative studies are rare. Our
530 work on the highly migratory Atlantic bluefin tuna is a compelling example of how
531 combining information from neutral and adaptive genetic markers with otolith
532 microchemistry data allows to triangulate towards a plausible hypothesis for the
533 evolution and demography of species with large populations sizes, long-distance
534 migrations and low genetic differentiation that make deciphering their populations
535 structure and connectivity patterns challenging.
536 Based on a comprehensive ABFT genome-wide SNPs dataset (including larvae from the
537 Slope Sea and spawning adults for the Mediterranean Sea and the Gulf of Mexico), we
538 confirm that current ABFT populations originated from two ancestral populations as
539 previously hypothesized (Rodríguez-Ezpeleta et al., 2019). Yet, these results also
540 revealed interbreeding in the Slope Sea and an eastern-western unidirectional trans-
541 Atlantic gene flow that challenges the assumption of two isolated spawning areas.
542 Moreover, the identification of previously unreported inter-specific introgressed regions
543 in the ABFT nuclear genome and potentially adaptive markers within a newly discovered
544 putative chromosomal inversion provided evidence to suggest that there have been
545 recent changes in ABFT connectivity which holds significant implications for the
546 conservation of the species.
547
548 *Strong admixture in the Slope Sea as the result of a potential source-sink dynamic*

549 The observed heterogeneously admixed genetic profiles of Slope Sea larvae and young
550 of the year ABFT support recurrent interbreeding between migrants from the Gulf of
551 Mexico and the Mediterranean Sea in the Slope Sea, which contributes to the admixed
552 genetic background of this spawning area. This observation is compatible with tagging
553 data, which shows adult individuals that enter the Gulf of Mexico or the Mediterranean
554 Sea also visit the Slope Sea spawning area during the potential spawning season (Aalto
555 et al., 2023; Block et al., 2005). Otolith microchemistry data provides evidence of
556 individuals with Mediterranean Sea and Gulf of Mexico origin compatible profiles in this
557 area (Siskey et al., 2016).

558 Our results on demographic history of the ABFT support that the Slope Sea
559 component originated from the Gulf of Mexico population, and that mixing with the
560 Mediterranean population started later. Thus, even if evidence of spawning activity in
561 the Slope Sea dates back to the 1950s (Baglin, 1976; Mather et al., 1995) and could have
562 started much earlier, it is most likely that the now observed genetic differentiation of
563 the Slope Sea is due to an increase in the immigration rates from the Mediterranean
564 component towards the Slope Sea. In fact, heterogeneous genetic profiles of individual
565 ABFT from the Slope Sea indicate a diverse genetic composition of spawners, a situation
566 at odds with the scenario of an exclusively self-sustained population at equilibrium.
567 Moreover, previous studies using otoliths have reported highly variable proportions of
568 Mediterranean origin individuals in the western Atlantic across the last five decades
569 (Kerr et al., 2020; Rooker et al., 2019; Secor et al., 2015; Siskey et al. 2016) and Puncher
570 et al. (2022) detected that the proportion of individuals genetically assigned to
571 Mediterranean origin increased over the past two decades at some northwestern

572 Atlantic areas, particularly among individuals younger than 15 years, which is
573 compatible with dynamically changing migratory trends.

574 Demographic connectivity is of major importance for fisheries management, as
575 it directly affects productivity and a stocks recruitment. Despite the limited knowledge
576 about the spawning dynamics in the Slope Sea, our data suggest asymmetrical genetic
577 connectivity towards the Slope Sea, possibly acting as a sink spawning area which is
578 receiving rather than exporting individuals, though its admixed nature could hamper the
579 detection of gene flow from the Slope Sea towards the Mediterranean Sea and the Gulf
580 of Mexico. This highlights the importance of understanding the demographic
581 interdependence of the Slope Sea with the other components, especially in view of
582 recent studies proposing the Slope Sea as a major spawning ground (Hernández et al.,
583 2022). One important knowledge gap is thus the understanding of Slope Sea born
584 individuals' life cycle. The currently observed genetic profiles are compatible with Slope
585 Sea born individuals showing (i) Slope Sea spawning-site fidelity, (ii) limited spawning,
586 (iii) spawning in the Gulf of Mexico and (iv) MED-like individuals born in the Slope Sea
587 spawning in the Mediterranean Sea. Unfortunately, weak genetic differentiation, typical
588 in marine fishes with large population sizes, together with the presence of intermediate
589 and heterogeneous (and presumably temporally variable in proportions) genetic profiles
590 hamper the clear identification of Slope Sea born individuals based solely on genetic
591 markers. Thus, we suggest that exploration of the dynamics of these individuals may
592 require the use of integrated methods, such as the combination of genetic markers with
593 otolith microchemistry (Brophy et al., 2020). The capability of identifying Slope Sea born
594 individuals and monitoring their presence across the ABFT distribution range, together
595 with an increase in larval sampling efforts in this spawning area, would allow us to obtain

596 and analyse temporal samples to understand their life cycle and estimate admixture
597 rates in the Slope Sea across generations.
598
599 *Evidence of the presence of Mediterranean origin fish in the Gulf of Mexico could*
600 *suggest recent changes in Atlantic bluefin tuna connectivity patterns*
601 Overall, our results support a historical split which originated two ancestrally
602 differentiated populations in the western Atlantic and Mediterranean spawning grounds
603 followed by a subsequent split between the Gulf of Mexico and Slope Sea and trans-
604 Atlantic unidirectional gene flow from the Mediterranean into western Atlantic
605 spawning grounds resulting in interbreeding in the Slope Sea and to a lesser extent in
606 the Gulf of Mexico. While admixture in the Slope Sea is reflected in the larval and
607 juvenile individual genetic profiles, larvae captured in the Gulf of Mexico were pure
608 GOM-like. Previous work suggested weak input of Mediterranean alleles in the larvae
609 collected from the western Gulf of Mexico in the year 2014 (Johnstone et al., 2021).
610 However, we have not detected evidence of such genetic connectivity in larval samples
611 from the western and eastern sides of the Gulf of Mexico collected before this date
612 (from years 2007 to 2010) despite using thousands of SNP genetic markers.
613 Nevertheless, the number of larvae collected in the Gulf of Mexico with individual
614 genetic profile available for this study remains limited (*n*=27) and the presence of MED-
615 like spawning adults suggests potential genetic connectivity between the
616 Mediterranean Sea and the Gulf of Mexico. Given that Slope Sea individuals' ancestry
617 proportions cover the range of MED-like individual genetic profiles, it would also be
618 possible that these MED-like individuals have their origin in the Slope Sea. The detection

of MED-like individuals in the Gulf of Mexico originating from the Slope Sea is made likely due to its proximity.

Due to the heterogeneous profile of the Slope Sea, the observed proportion of MED-like individuals in the Gulf of Mexico originated in the Slope Sea could only be explained by a high number of Slope Sea MED-like individuals entering the Gulf of Mexico, unless MED-like individuals originated in the Slope Sea under a scenario of even higher inflow from the eastern Atlantic. Otolith microchemistry analyses revealed that genetically MED-like individuals captured in the Gulf of Mexico showed an otolith isotopic composition of oxygen ($\delta^{18}O$) intermediate between the Gulf of Mexico and the Mediterranean spawning areas, suggesting that these were probably not born in the Gulf of Mexico. Interestingly, these intermediate values are consistent with the proposed signature range of a potential third contingent, compatible with a Slope Sea or Mediterranean origin of individuals showing early and/or more intense migratory behaviour (Brophy et al., 2020). These observations allow for different possible origins of the MED-like individuals captured in the Gulf of Mexico. Additional observations of the genetic composition of adult ABFT spawning in the Slope Sea coupled with further knowledge about the migratory behaviour of Mediterranean ABFT would be needed to assign the origin of these MED-like individuals more accurately.

Regardless of the origin of the MED-like individuals in the Gulf of Mexico, a few dozen migrants exchanged per generation, if effectively spawning and not affected by negative selection, is theoretically sufficient to erase genetic differentiation between populations (Gagnaire et al., 2015; Lowe & Allendorf, 2010; Waples, 1998). The low F_{ST} values reported in this study are common among marine fishes with large population sizes, high dispersal rates and wide-ranging distributions (da Fonseca et al., 2022;

643 Fuentes-Pardo et al., 2023; Hauser & Carvalho, 2008). While genetic differentiation of
644 ABFT between the Mediterranean Sea and the Gulf of Mexico could persist despite
645 admixed individuals in the Slope Sea, the number of migrants detected in the Gulf of
646 Mexico is theoretically expected to lead to genetic homogeneity between eastern and
647 western born ABFT and is thus not easily compatible with significant F_{ST} values.
648 Histological inspection confirmed the presence of at least one MED-like female which
649 had spawned less than 48 h before capture in the Gulf of Mexico, suggesting that MED-
650 like individuals spawn in the Gulf of Mexico. One possible explanation for the observed
651 levels of genetic differentiation would be negative selection against Mediterranean
652 genes preventing successful gene flow. Hence, we have explored different sources of
653 genetic variation, which could help to explain the maintenance of genetic differentiation
654 between highly demographically connected populations. More specifically, we have
655 explored the effect of locally adaptive alleles, which could maintain genetic
656 differentiation in the presence of gene flow (Tigano & Friesen, 2016) and inter-specific
657 introgression, which can trigger different evolutionary processes, such as the input of
658 adaptive alleles (Huerta-Sánchez et al., 2014) or the contribution to reproductive
659 isolation (Duranton et al., 2020). However, we did not find evidence to confirm the
660 maintenance of genetic differentiation through either local adaptation or reproductive
661 isolation. These would lead to much higher levels of F_{ST} at loci involved in
662 incompatibilities and/or selection than the ones observed in this work. Besides,
663 genome-wide and homogeneously distributed genetic differentiation between
664 Mediterranean Sea and Gulf of Mexico reference individuals at neutral alleles reflects
665 that differentiation is not primarily driven by introgression or adaptation, but by the
666 effect of historical long-term isolation between Mediterranean and Atlantic populations,

667 as indicated by their inferred demographic history. Moreover, interbreeding in the Slope
668 Sea implies genetic compatibility between GOM-like and MED-like individuals, which
669 makes the barrier to gene flow hypothesis unlikely to explain the maintenance of genetic
670 differentiation. Another possibility is that selection undetected in this study impedes
671 incorporation of MED-like alleles in the Gulf of Mexico. On the one hand, widespread
672 polygenic selection remains difficult to reject based on outlier detection tests as the
673 ones used here, as these are underpowered to detect weakly selected loci, though
674 genetic differences are unlikely maintained by weak polygenic selection in the presence
675 of gene flow. On the other hand, the use of reduced representation sequencing could
676 lead to missed localized selective sweeps. Analyses based on whole genome sequencing
677 data would allow one to detect adaptation signals missed in our study. Alternatively, we
678 propose that the currently observed ancestry patterns could be explained by recent
679 secondary contact following genetic divergence of both ancestral populations after long-
680 term isolation with reduced or no migration, and that the high observed migration rates,
681 in the absence of barriers to gene flow and if sustained over time, could ultimately lead
682 to genetic homogenization and the consequently the loss of genetic differentiation.
683
684 *Possible drivers and implications of changes in inter-spawning area connectivity*
685 The observed levels of genetic differentiation, hardly compatible with the high level of
686 gene flow suggested by our results in constant equilibrium, suggest that connectivity
687 patterns between ABFT spawning grounds could be subjected to temporal changes and
688 that an increase in migration from the Mediterranean Sea towards the known western
689 Atlantic spawning areas could have a genetic homogenizing effect. Such a homogenizing
690 effect is expected to be correlated with migration rates and the effective population size

691 (Ne) of the recipient population (Gagnaire et al., 2015; Lowe & Allendorf, 2010), which
692 in turn relates to the number of adult individuals among other factors (Waples, 2022)
693 and would consequently be affected by fluctuations in the population's abundance. The
694 abundance of ABFT stocks have undergone strong changes during the last ~60 years.
695 After both the western and the eastern Atlantic stocks reached a critical status, including
696 the collapse of several fisheries around the 1960-1970s (Fromentin, 2009; Porch et al.,
697 2019), the western Atlantic stock has not recovered as rapidly as the eastern Atlantic
698 stock (of Mediterranean origin), whose estimated abundance has been one order of
699 magnitude larger for several decades (ICCAT, 2017), despite decades of conservation
700 efforts. This slow recovery could result from a regime shift over the last decades, due to
701 the combination of oceanographic changes in the equatorial Atlantic and overfishing
702 (Fromentin, Reygondeau, et al., 2014) possibly affecting both migration rates and
703 effective population sizes. Fluctuations in the abundance and distribution of eastern
704 ABFT during the last century were largely explained by the Atlantic Multi-decadal
705 Oscillation (AMO) (Faillettaz et al., 2019) and long-term trends in temperature (Ravier &
706 Fromentin, 2004). Moreover, coinciding with the last negative AMO period starting in
707 the 1960s, ABFT had disappeared from several North-East Atlantic areas where it is
708 reappearing during the current positive AMO phase starting in the mid-1990s (Aarestrup
709 et al., 2022; Horton et al., 2020; Nøttestad et al., 2020). Furthermore, increasing catches
710 of ABFT in Greenland waters show that the northern limit of ABFT distribution was
711 expanded northwards during the last decade by mostly individuals of Mediterranean
712 genetic origin (Jansen et al., 2021). Based on electronic tagging data, the proportion of
713 individuals of eastern origin present in the western Atlantic has also increased during
714 the last two decades (Aalto et al., 2021). Interestingly, AMO positive or warm phases as

715 well as current global warming involve an increase in habitat suitability in most of these
716 northern areas (Faillettaz et al., 2019; Fromentin, Reygondeau, et al., 2014). In summary,
717 ABFT populations' sizes, distribution and migratory behaviour have been undergoing
718 changes during the last decades, probably due to changes in environmental conditions,
719 fishing pressure, conservation efforts or combined effects of these that have affected
720 populations in different manners. These changes could explain migration intensification
721 from the recently expanded eastern stock towards the more slowly recovering western
722 Atlantic stock. Our analyses support that the recent short-term genetic effects of
723 immigration on the variance in ancestries are much stronger in the Slope Sea than in the
724 Gulf of Mexico. This could be due to behavioural preferences or favourable conditions
725 which would make it easier for Mediterranean individuals to reach and reproduce in the
726 Slope Sea, or due to a smaller effective population size compared to the Gulf of Mexico.
727 May westward migration rates be consequently strongly increasing, the homogenizing
728 effect of this unidirectional migration would ultimately lead to the genetic swamping of
729 the GOM-like genetic component. It is thus possible that genetic differentiation is
730 detected in the existing samples because gene flow is relatively recent relative to mean
731 generation times estimated to average 9.6 years for the western stock (Collette et al.,
732 2011), and that this genetic divergence will be attenuated across generations in the
733 future. While genetic connectivity does not necessarily equate with demographic
734 dependence, genetic erosion would not necessarily imply demographic decline either,
735 but could have more unpredictable demographic consequences.
736
737 *Inter-specific gene introgression from albacore to Atlantic bluefin tuna*

738 We detected for the first-time signatures of introgression from albacore tuna in the
739 nuclear genome of the ABFT, which contradicts a previous report (Ciezarek et al., 2018).
740 For the D-statistic analysis, the Southern bluefin tuna was used as an out-group clade to
741 define the ancestral state, which could not be accurate according to a previous study on
742 the phylogeny of the genus (Díaz-Arce et al., 2016), potentially biasing the results,
743 especially if historical introgression events among the explored species involved the
744 Southern bluefin tuna. However, TreeMix analysis, for which no assumption on the
745 ancestral state were made, did not revealed such gene-flow events even when
746 increasing the number of allowed migration events to five. This, together with the
747 consistency between both analyses based on the nuclear genome and the proportion of
748 mitochondrial introgressed ABFT individuals across spawning areas, support the validity
749 of the Southern bluefin tuna as an out-group for the ABBA/BABA tests performed in this
750 work. The most probable inter-lineage gene flow event estimated by the TreeMix
751 analysis happened between the albacore and the ABFT Mediterranean population. The
752 presence of mitochondrial introgression has also been reported in PBFT (Chow &
753 Kishino, 1995); however, although we included very few PBFT samples, we did not find
754 any sign of nuclear introgression in this species. Considering that ABFT and PBFT evolved
755 from a recent common ancestor (Díaz-Arce et al., 2016) and that they show very little
756 genetic divergence, our results suggest that introgression between albacore tuna and
757 ABFT happened after the split between the ABFT and PBFT lineages. Thus, to explain the
758 presence of albacore-like mitochondrial genomes in PBFT, we hypothesize either
759 parallel introgression events between albacore tuna and both ABFT and PBFT, or that
760 mitochondrial introgressed genomes present in PBFT have been introgressed through
761 genetic exchanges with the ABFT. Likewise, among ABFT individuals, the signal of

762 introgression from albacore is stronger in the Mediterranean and the Slope Sea and
763 nearly absent in the Gulf of Mexico. The gradient of albacore ancestry in ABFT spawning
764 areas further suggests that this introgression occurred (or has been more intense) in the
765 Mediterranean ABFT population, where the signal at the nuclear genome is strongest
766 and where spawning areas for both species overlap (Alemany et al. 2010), and then
767 diffused towards the Slope Sea and to a lesser extent the Gulf of Mexico through
768 multigenerational gene flow. These different introgression signal intensities from east
769 to west support gene flow between the Mediterranean Sea and Slope Sea spawning
770 components, which is in accordance with the admixed nature of Slope Sea individuals.
771 Besides, the nearly complete absence of both nuclear and mitochondrial introgression
772 in Gulf of Mexico individuals suggests that introgression happened after the split
773 between MED-like and GOM-like ancestral lineages and is consistent with the inferred
774 scenario of historically restricted gene flow from the Mediterranean Sea to the Gulf of
775 Mexico, which contrasts with the frequency of MED-like spawners observed in the Gulf
776 of Mexico. Overall, the east-west gradient of introgressed albacore alleles confirms the
777 inferred connectivity patterns presented in this study. However, this together with the
778 fact that the contribution of albacore introgression to genetic differentiation between
779 Mediterranean Sea and Gulf of Mexico ABFT populations appears to be limited at best
780 and therefore it could contribute but not explain the maintenance of genetic
781 differentiation between MED-like and GOM-like individuals, strongly suggests that other
782 mechanisms, such as local adaptation, maintain genetic differentiation in the presence
783 of gene flow, or that migration towards the Gulf of Mexico has increased recently. We
784 identified a particular genomic region with characteristics typical of a chromosomal
785 inversion, such as high linkage disequilibrium and increased heterozygosity values in

786 samples occupying intermediate positions in a local PCA (Barth et al., 2019; Jiménez-
787 Mena et al., 2020; Puncher et al., 2019), through outlier variant scan analysis. Our
788 analysis supports that, as reported for other species (Jay et al., 2018), the origin of this
789 inversion was introduced into the ABFT genome as the result of a past introgression
790 event from albacore tuna. This region aggregates a high number of outlier genetic
791 markers. However, high linkage disequilibrium could bias towards the detection of false
792 positives within this region due to the synergic signal of dozens of variants. With the aim
793 of making the least possible assumptions, the a priori grouping of individuals required
794 by the method for outlier detection implemented in BayeScan was made based on
795 location. Not excluding MED-like individuals captured in the Gulf of Mexico could lead
796 to type I errors. Because we were more interested in reducing the risk of type I error,
797 we applied relaxed filters for candidate outlier loci selection and also considered outliers
798 detected by a complementary method where no assumptions were made. We could not
799 associate the presence of this introgression nor chromosomal inversion with ecological
800 or environmental factors; yet, introgression represents an important source of genetic
801 adaptive variation playing an important role favouring speciation through processes
802 such as introgression of favoured alleles (Arnold & Martin, 2009; Clarkson et al., 2014;
803 Hedrick, 2013) or reproductive isolation (Abbott et al., 2013; Duranton et al., 2020).
804 Moreover, the literature abounds with examples showing that chromosomal inversions
805 are associated with local adaptation in the presence of gene flow (Barth, Berg, et al.,
806 2017; Berg et al., 2016; Huang et al., 2020; Le Moan et al., 2021; Mérot et al., 2021;
807 Thorstensen et al., 2022; Wellenreuther & Bernatchez, 2018). Given that allele
808 frequency differences between the Mediterranean and the Gulf of Mexico components
809 are stronger in the candidate chromosomal inversion than the mean genome-wide

differentiation, ascertaining its role in the ABFT adaptation could be of great relevance to understand the species resilience to the already predicted changes in environmental conditions (Erauskin-Extramiana et al., 2019; Muhling et al., 2011).

Implications for Atlantic bluefin tuna conservation and management

Conservation of ABFT is challenged by past and future fishing pressure (Fromentin, Bonhommeau, et al., 2014; Secor et al., 2015), which has sharply increased since 2018 following the rebuilding of the Mediterranean ABFT population (ICCAT, 2023), and by changes in environmental conditions (often interacting with fishing pressure), which have been shown to alter population size and productivity, migratory behaviour and spatial distribution (Ravier & Fromentin, 2004). From a conservation perspective, hybridization between genetically differentiated lineages, in this case between GOM-like and MED-like individuals, could increase each population's genetic diversity, leading to the incorporation of potentially adaptive genomic variation and reducing vulnerability to environmental changes (Brauer et al., 2023). However, strong unidirectional gene flow could provoke genetic swamping of the western Atlantic spawning areas jeopardizing ABFT genetic diversity (Roberts et al., 2010). In this sense, large effective population sizes, which could increase following a rebuilding of abundance at the different spawning areas (Hoey et al., 2022) would counteract the homogenizing effect of genetic drift. In the absence of accurate estimations of ABFT effective populations sizes (Puncher et al., 2018), further genetic monitoring of temporal samples could help to understand potential ongoing trends in genetic diversity conservation (Hoban et al., 2014; Oosting et al., 2019).

From a fisheries management perspective, the confirmation of ongoing admixture in the Slope Sea challenges the paradigm of two isolated ABFT stocks. However, large knowledge gaps related to the dynamics of Slope Sea individuals, the magnitude of the Slope Sea spawning in terms of recruitment, and its demographic connectivity with other components hinder explicit modelling of it as a distinct stock. Nonetheless, the recently adopted management procedure (ICCAT, 2023) does explicitly consider spawning in the Slope Sea. Our study highlights the need for further monitoring combining multidisciplinary data such as larval sampling, tagging, otolith microchemistry signature and genetic origin to understand the Slope Sea population dynamics and the relevance of this spawning area in demographic and evolutionary terms.

Author contributions

NDA, HA and NRE designed research. NDA, PAG, SAH, AP and NRE contributed analytical tools. DER, JFW, PA, FA, RA, SD, ARH, FSK, JMQ and JRR contributed samples. NDA analysed data. NDA, PAG, DER, JFW, SAH, JMF, DB, ML, IF, NG, JR, HA and NRE interpreted data. NDA wrote the article, with insightful contributions from all authors. All authors revised the manuscript and agreed with its publication.

Acknowledgements

We thank all the participants of the GBYP biological sampling programme, in particular Naiara Serrano, Xiker Salaberria and Inma Martín for tissue sample handling and storage, Iraide Artetxe-Arrate and Ai Kimoto for database management and Iñaki Mendibil and Elisabete Bilbao for excellent laboratory work. We also thank Marty Kardos for his valuable comments, contributing to the quality improvement of this manuscript. This

study has been carried out under the provision of the ICCAT Atlantic Wide Research Program for Bluefin Tuna (GBYP), funded by the European Community (Grant SI2/542789), Canada, Croatia, Japan, Norway, Turkey, the United States (NMFS NA11NMF4720107), Chinese Taipei and the ICCAT Secretariat. This work was also supported by a grant (project GENGES) and a pre-doctoral fellowship to ND-A, from the Department of Agriculture and Fisheries of the Basque Government. The contents of the article do not necessarily reflect the point of view of ICCAT or of the other funders. This manuscript is contribution number 1186 from the Marine Research Division of AZTI.

Data Availability Statement

De-multiplexed sequences are deposited in the SRA (Bioproject PRJNA804694). Scripts used to perform the analyses described in this manuscript can be found at https://github.com/rodriguez-ezpeleta/ABFT_popgentrace.

Benefit-Sharing Statement

This research is a result of a collaborative agreement between partners which are all included as co-authors. Each partner respected the Nagoya Protocol on Access and benefit-sharing entered into force on the 12 October 2014 produced by the United Nations Convention on Biological Diversity to carry out its activities under this Agreement and performed the necessary formalities to the competent authorities.

Ethics statement

Fish samples used in this study were provided by fisheries and therefore there are no ethical guidelines applicable.

Declaration of Interests

The authors declare no competing interests.

References

Aalto, E. A., S. Dedman, M. J. W. Stokesbury, R. J. Schallert, M. Castleton, and B. A. Block. 2023. Evidence of bluefin tuna (*Thunnus thynnus*) spawning in the Slope Sea region of the Northwest Atlantic from electronic tags. ICES Journal of Marine Science., 80, 861-877.

Aalto, E. A., F. Ferretti, M. V. Lauretta, J. F. Walter, M. J. W. Stokesbury, R. J. Schallert, and B. A. Block. 2021. Stock-of-origin catch estimation of Atlantic bluefin tuna (Thunnus thynnus) based on observed spatial distributions. Canadian Journal of Fisheries and Aquatic Sciences **78**:1193-1204.

Aarestrup, K., H. Baktoft, K. Birnie-Gauvin, A. Sundelöf, M. Cardinale, G. Quilez-Badia, I. Onandia, M. Casini, E. E. Nielsen, A. Koed, F. Alemany, and B. R. MacKenzie. 2022. First tagging data on large Atlantic bluefin tuna returning to Nordic waters suggest repeated behaviour and skipped spawning. Scientific Reports **12**:11772.

Abbott, R., D. Albach, S. Ansell, J. W. Arntzen, S. J. E. Baird, N. Bierne, J. Boughman, A. Brelsford, C. A. Buerkle, R. Buggs, R. K. Butlin, U. Dieckmann, F. Eroukhmanoff, A. Grill, S. H. Cahan, J. S. Hermansen, G. Hewitt, A. G. Hudson, C. Jiggins, J. Jones, B. Keller, T. Marczewski, J. Mallet, P. Martinez-Rodriguez, M. Möst, S. Mullen, R. Nichols, A. W. Nolte, C. Parisod, K. Pfennig, A. M. Rice, M. G. Ritchie, B. Seifert, C. M. Smadja, R. Stelkens, J. M. Szymura, R. Väinölä, J. B. W. Wolf, and D. Zinner. 2013. Hybridization and speciation. Journal of Evolutionary Biology **26**:229-246.

Alemany, F., L. Quintanilla, P. Velez-Belchí, A. García, D. Cortés, J. M. Rodríguez, M. L. Fernández de Puelles, C. González-Pola, and J. L. López-Jurado. 2010. Characterization of the spawning habitat of Atlantic bluefin tuna and related species in the Balearic Sea (western Mediterranean). Progress in Oceanography **86**:21-38.

Alexander, D. H., J. Novembre, and K. Lange. 2009. Fast model-based estimation of ancestry in unrelated individuals. Genome Research, 19, 1655-1664.

Alvarado Bremer, J. R., J. Viñas, J. Mejuto, B. Ely, and C. Pla. 2005. Comparative phylogeography of Atlantic bluefin tuna and swordfish: the combined effects of vicariance, secondary contact, introgression, and population expansion on the regional phylogenies of two highly migratory pelagic fishes. Molecular Phylogenetics and Evolution **36**:169-187.

Aranda, G., L. Aragón, A. Corriero, C. C. Mylonas, F. d. la Gándara, A. Belmonte, and A. Medina. 2011. GnRHa-induced spawning in cage-reared Atlantic bluefin tuna: An evaluation using stereological quantification of ovarian post-ovulatory follicles. Aquaculture **317**:255-259.

Arnold, M. L., and N. H. Martin. 2009. Adaptation by introgression. Journal of Biology **8**:82.

Arregui, I., B. Galuardi, N. Goñi, C. H. Lam, I. Fraile, J. Santiago, M. Lutcavage, and H. Arrizabalaga. 2018. Movements and geographic distribution of juvenile bluefin tuna in the Northeast Atlantic, described through internal and satellite archival tags. ICES Journal of Marine Science **75**:1560-1572.

Baglin, R. 1976. A preliminary study of the gonadal development and fecundity of the western Atlantic bluefin tuna. Collective Volume of Scientific Papers ICCAT **5**:279-289.

Barth, J. M. I., P. R. Berg, P. R. Jonsson, S. Bonanomi, H. Corell, J. Hemmer-Hansen, K. S. Jakobsen, K. Johannesson, P. E. Jorde, H. Knutsen, P.-O. Moksnes, B. Star, N. C. Stenseth, H. Svedäng, S. Jentoft, and C. André. 2017. Genome architecture enables local adaptation of Atlantic cod despite high connectivity. Molecular Ecology **26**:4452-4466.

Barth, J. M. I., M. Damerau, M. Matschiner, S. Jentoft, and R. Hanel. 2017. Genomic Differentiation and Demographic Histories of Atlantic and Indo-Pacific Yellowfin Tuna (Thunnus albacares) Populations. Genome Biology and Evolution **9**:1084-1098.

Barth, J. M. I., D. Villegas-Ríos, C. Freitas, E. Moland, B. Star, C. André, H. Knutsen, I. Bradbury, J. Dierking, C. Petereit, D. Righton, J. Metcalfe, K. S. Jakobsen, E. M. Olsen, and S. Jentoft. 2019. Disentangling structural genomic and behavioural barriers in a sea of connectivity. Molecular Ecology **28**:1394-1411.

Begg, G. A., K. D. Friedland, and J. B. Pearce. 1999. Stock identification and its role in stock assessment and fisheries management: an overview. Fisheries Research **43**:1-8.

Berg, P. R., B. Star, C. Pampoulie, M. Sodeland, J. M. I. Barth, H. Knutsen, K. S. Jakobsen, and S. Jentoft. 2016. Three chromosomal rearrangements promote genomic divergence between migratory and stationary ecotypes of Atlantic cod. Scientific Reports **6**:23246.

Bernatchez, L. 2016. On the maintenance of genetic variation and adaptation to environmental change: considerations from population genomics in fishes. Journal of Fish Biology **89**:2519-2556.

Bernatchez, L., M. Wellenreuther, C. Araneda, D. T. Ashton, J. M. I. Barth, T. D. Beacham, G. E. Maes, J. T. Martinsohn, K. M. Miller, K. A. Naish, J. R. Ovenden, C. R. Primmer, H. Young Suk, N. O. Therkildsen, and R. E. Withler. 2017. Harnessing the Power of Genomics to Secure the Future of Seafood. Trends in Ecology & Evolution **32**:665-680.

Block, B. A., S. L. H. Teo, A. Walli, A. Boustany, M. J. W. Stokesbury, C. J. Farwell, K. C. Weng, H. Dewar, and T. D. Williams. 2005. Electronic tagging and population structure of Atlantic bluefin tuna. Nature **434**:1121-1127.

Bonanomi, S., L. Pellissier, N. O. Therkildsen, R. B. Hedeholm, A. Retzel, D. Meldrup, S. M. Olsen, A. Nielsen, C. Pampoulie, J. Hemmer-Hansen, M. S. Wisz, P. Grønkjær, and E. E. Nielsen. 2015. Archived DNA reveals fisheries and climate induced collapse of a major fishery. Scientific Reports **5**:15395.

Brauer, C. J., J. Sandoval-Castillo, K. Gates, M. P. Hammer, P. J. Unmack, L. Bernatchez, and L. B. Beheregaray. 2023. Natural hybridization reduces vulnerability to climate change. Nature Climate Change **13**:282-289.

Brophy, D., N. Rodríguez-Ezpeleta, I. Fraile, and H. Arrizabalaga. 2020. Combining genetic markers with stable isotopes in otoliths reveals complexity in the stock structure of Atlantic bluefin tuna (Thunnus thynnus). Scientific Reports **10**:14675.

Brown-Peterson, N. J., D. M. Wyanski, F. Saborido-Rey, B. J. Macewicz, and S. K. Lowerre-Barbieri. 2011. A Standardized Terminology for Describing Reproductive Development in Fishes. Marine and Coastal Fisheries **3**:52-70.

Cadrin, L. A. Kerr, and S. Mariani, editors. Stock Identification Methods (Second Edition) (pp. 297–327). Academic Press, San Diego.

Chow, S., and H. Kishino. 1995. Phylogenetic relationships between tuna species of the genus Thunnus (Scombridae: Teleostei): Inconsistent implications from morphology, nuclear and mitochondrial genomes. Journal of Molecular Evolution **41**:741-748.

Ciezarek, A. G., O. G. Osborne, O. N. Shipley, E. J. Brooks, S. R. Tracey, J. D. McAllister, L. D. Gardner, M. J. E. Sternberg, B. Block, and V. Savolainen. 2018. Phylotranscriptomic

Insights into the Diversification of Endothermic Thunnus Tunas. Molecular Biology and Evolution **36**:84-96.
Clarkson, C. S., D. Weetman, J. Essandoh, A. E. Yawson, G. Maslen, M. Manske, S. G. Field, M. Webster, T. Antão, B. MacInnis, D. Kwiatkowski, and M. J. Donnelly. 2014. Adaptive introgression between Anopheles sibling species eliminates a major genomic island but not reproductive isolation. Nature Communications **5**:4248.
Collette, B. B., K. E. Carpenter, B. A. Polidoro, M. J. Juan-Jordá, A. Boustany, D. J. Die, C. Elfes, W. Fox, J. Graves, L. R. Harrison, R. McManus, C. V. Minte-Vera, R. Nelson, V. Restrepo, J. Schratwieser, C.-L. Sun, A. Amorim, M. Brick Peres, C. Canales, G. Cardenas, S.-K. Chang, W.-C. Chiang, N. de Oliveira Leite, H. Harwell, R. Lessa, F. L. Fredou, H. A. Oxenford, R. Serra, K.-T. Shao, R. Sumaila, S.-P. Wang, R. Watson, and E. Yáñez. 2011. High Value and Long Life - Double Jeopardy for Tunas and Billfishes. Science **333**:291-292.
da Fonseca, R., P. Campos, A. Rey de la Iglesia, G. Barroso, L. Bergeron, M. Nande, F. Tuya, S. Abidli, M. Pérez, I. Riveiro, P. Carrera, A. Jurado-Ruzafa, M. T. G. Santamaria, R. Faria, A. Machado, M. Fonseca, E. Froufe, and L. F. C. Castro. 2022. Population genomics reveals the underlying structure of the small pelagic European sardine and suggests low connectivity within Macaronesia. Authorea. https://doi.org/10.22541/au.161628445.52373083/v3
Díaz-Arce, N., H. Arrizabalaga, H. Murua, X. Irigoien, and N. Rodríguez-Ezpeleta. 2016. RAD-seq derived genome-wide nuclear markers resolve the phylogeny of tunas. Molecular Phylogenetics and Evolution **102**:202-207.
Durand, E. Y., N. Patterson, D. Reich, and M. Slatkin. 2011. Testing for ancient admixture between closely related populations. Molecular Biology and Evolution **28**:2239-2252.
Duranton, M., F. Allal, S. Valière, O. Bouchez, F. Bonhomme, and P.-A. Gagnaire. 2020. The contribution of ancient admixture to reproductive isolation between European sea bass lineages. Evolution Letters **4**:226-242.
Erauskin-Extramiana, M., H. Arrizabalaga, A. J. Hobday, A. Cabré, L. Ibaibarriaga, I. Arregui, H. Murua, and G. Chust. 2019. Large-scale distribution of tuna species in a warming ocean. Global Change Biology **25**:2043-2060.
Etter, P. D., S. Bassham, P. A. Hohenlohe, E. A. Johnson, and W. A. Cresko. 2012. SNP discovery and genotyping for evolutionary genetics using RAD sequencing. Pages 157-178, In V. Orgogozo & M. Rockman (Eds.), Molecular methods for evolutionary genetics. Springer.
Faillettaz, R., G. Beaugrand, E. Goberville, and R. R. Kirby. 2019. Atlantic Multidecadal Oscillations drive the basin-scale distribution of Atlantic bluefin tuna. Science Advances **5**:eaar6993.
Foll, M., and O. Gaggiotti. 2008. A Genome-Scan Method to Identify Selected Loci Appropriate for Both Dominant and Codominant Markers: A Bayesian Perspective. Genetics **180**:977-993.
Fraser, D. J., and L. Bernatchez. 2001. Adaptive evolutionary conservation: towards a unified concept for defining conservation units. Molecular Ecology **10**:2741-2752.
Fromentin, J.-M. 2009. Lessons from the past: investigating historical data from bluefin tuna fisheries. Fish and Fisheries **10**:197-216.
Fromentin, J.-M., S. Bonhommeau, H. Arrizabalaga, and L. T. Kell. 2014a. The spectre of uncertainty in management of exploited fish stocks: The illustrative case of Atlantic bluefin tuna. Marine Policy **47**:8-14.
Fromentin, J.-M., and J. E. Powers. 2005. Atlantic bluefin tuna: population dynamics, ecology, fisheries and management. Fish and Fisheries **6**:281-306.
Fromentin, J.-M., G. Reygondeau, S. Bonhommeau, and G. Beaugrand. 2014b. Oceanographic changes and exploitation drive the spatio-temporal dynamics of Atlantic bluefin tuna (Thunnus thynnus). Fisheries Oceanography **23**:147-156.

Fuentes-Pardo, A. P., E. D. Farrell, M. E. Pettersson, C. G. Sprehn, and L. Andersson. 2023. The genomic basis and environmental correlates of local adaptation in the Atlantic horse mackerel (Trachurus trachurus). Evolutionary Applications, 16, 1201–1219.
Gagnaire, P.-A., T. Broquet, D. Aurelle, F. Viard, A. Souissi, F. Bonhomme, S. Arnaud-Haond, and N. Bierne. 2015. Using neutral, selected, and hitchhiker loci to assess connectivity of marine populations in the genomic era. Evolutionary Applications **8**:769-786.
Galuardi, B., F. Royer, W. Golet, J. Logan, J. Neilson, and M. Lutcavage. 2010. Complex migration routes of Atlantic bluefin tuna (Thunnus thynnus) question current population structure paradigm. Canadian Journal of Fisheries and Aquatic Sciences **67**:966-976.
Green, R. E., J. Krause, A. W. Briggs, T. Maricic, U. Stenzel, M. Kircher, N. Patterson, H. Li, W. Zhai, and M. H.-Y. Fritz. 2010. A draft sequence of the Neandertal genome. Science **328**:710-722.
Gutenkunst, R. N., R. D. Hernandez, S. H. Williamson, and C. D. Bustamante. 2009. Inferring the joint demographic history of multiple populations from multidimensional SNP frequency data. PLoS genetics **5**:e1000695.
Hauser, L., and G. R. Carvalho. 2008. Paradigm shifts in marine fisheries genetics: ugly hypotheses slain by beautiful facts. Fish and Fisheries **9**:333-362.
Hedrick, P. W. 2013. Adaptive introgression in animals: examples and comparison to new mutation and standing variation as sources of adaptive variation. Molecular Ecology **22**:4606-4618.
Hernández, C. M., D. E. Richardson, I. I. Rypina, K. Chen, K. E. Marancik, K. Shulzitski, and J. K. Llopiz. 2022. Support for the Slope Sea as a major spawning ground for Atlantic bluefin tuna: evidence from larval abundance, growth rates, and particle-tracking simulations. Canadian Journal of Fisheries and Aquatic Sciences **79**:814-824.
Hoban, S., J. A. Arntzen, M. W. Bruford, J. A. Godoy, A. Rus Hoelzel, G. Segelbacher, C. Vilà, and G. Bertorelle. 2014. Comparative evaluation of potential indicators and temporal sampling protocols for monitoring genetic erosion. Evolutionary Applications **7**:984-998.
Hoey, J. A., K. W. Able, and M. L. Pinsky. 2022. Genetic decline and recovery of a demographically rebuilt fishery species. Molecular Ecology **31**:5684-5698.
Hoffmann, A. A., and C. M. Sgrò. 2011. Climate change and evolutionary adaptation. Nature **470**:479-485.
Horton, T. W., B. A. Block, A. Drumm, L. A. Hawkes, M. O'Cuaig, N. Ó. Maoiléidigh, R. O'Neill, R. J. Schallert, M. J. W. Stokesbury, and M. J. Witt. 2020. Tracking Atlantic bluefin tuna from foraging grounds off the west coast of Ireland. ICES Journal of Marine Science **77**:2066-2077.
Huang, K., R. L. Andrew, G. L. Owens, K. L. Ostevik, and L. H. Rieseberg. 2020. Multiple chromosomal inversions contribute to adaptive divergence of a dune sunflower ecotype. Molecular Ecology **29**:2535-2549.
Huerta-Sánchez, E., X. Jin, Asan, Z. Bianba, B. M. Peter, N. Vinckenbosch, Y. Liang, X. Yi, M. He, M. Somel, P. Ni, B. Wang, X. Ou, Huasang, J. Luosang, Z. X. P. Cuo, K. Li, G. Gao, Y. Yin, W. Wang, X. Zhang, X. Xu, H. Yang, Y. Li, J. Wang, J. Wang, and R. Nielsen. 2014. Altitude adaptation in Tibetans caused by introgression of Denisovan-like DNA. Nature **512**:194-197.
Hutchinson, W. F. 2008. The dangers of ignoring stock complexity in fishery management: the case of the North Sea cod. Biology Letters **4**:693-695.
ICCAT. 2023. Recommendation by ICCAT establishing a management procedure for Atlantic Bluefin tuna to be used for both the Western Atlantic and Eastern Atlantic and Mediterranean management areas. Page 8, https://www.iccat.int/Documents/Recs/compendiopdf-e/2022-09-e.pdf.
ICCAT, S. 2017. Report of the Standing Committee on Research and Statistics (SCRS), Madrid, Spain, 2017. ICCAT. https://www.iccat.int/Documents/Meetings/Docs/2017_SCRS_REP_ENG.pdf

ICCAT, S. 2019. Report of the Standing Committee on Resarch and Statistics (SCRS), Madrid, Spain, 2019. http://www.iccat.int/Documents/Meetings/Docs/2019/REPORTS/2019_SCRS_ENG.pdf

ICCAT, S. 2021. 2020 SRCS Advice to the Comission. ICCAT, https://www.iccat.int/Documents/BienRep/REP_EN_20-21_I-1.pdf.

ICCAT. 2023. Recommendation by ICCAT establishing a management procedure for Atlantic Bluefin Tuna to be used for both the Western Atlantic and Eastern Atlantic and Mediterranean management areas. Page 8. https://www.iccat.int/Documents/Recs/compendiopdf-ecompendiopdfe/2022-09-e.pdf.

Jansen, T., E. E. Nielsen, N. Rodriguez-Ezpeleta, H. Arrizabalaga, S. Post, and B. R. MacKenzie. 2021. Atlantic bluefin tuna (Thunnus thynnus) in Greenland — mixed-stock origin, diet, hydrographic conditions, and repeated catches in this new fringe area. Canadian Journal of Fisheries and Aquatic Sciences **78**:400-408.

Jay, P., A. Whibley, L. Frézal, M. Á. Rodríguez de Cara, R. W. Nowell, J. Mallet, K. K. Dasmahapatra, and M. Joron. 2018. Supergene Evolution Triggered by the Introgression of a Chromosomal Inversion. Current Biology **28**:1839-1845.e1833.

Jiménez-Mena, B., A. Le Moan, A. Christensen, M. van Deurs, H. Mosegaard, J. Hemmer-Hansen, and D. Bekkevold. 2020. Weak genetic structure despite strong genomic signal in lesser sandeel in the North Sea. Evolutionary Applications **13**:376-387.

Johnstone, C., M. Pérez, E. Malca, J. M. Quintanilla, T. Gerard, D. Lozano-Peral, F. Alemany, J. Lamkin, A. García, and R. Laiz-Carrión. 2021. Genetic connectivity between Atlantic bluefin tuna larvae spawned in the Gulf of Mexico and in the Mediterranean Sea. PeerJ **9**:e11568.

Jombart, T., and I. Ahmed. 2011. adegenet 1.3-1: new tools for the analysis of genome-wide SNP data. Bioinformatics **27**:3070-3071.

Kerr, L. A., N. T. Hintzen, S. X. Cadrin, L. W. Clausen, M. Dickey-Collas, D. R. Goethel, E. M. C. Hatfield, J. P. Kritzer, and R. D. M. Nash. 2016. Lessons learned from practical approaches to reconcile mismatches between biological population structure and stock units of marine fish. ICES Journal of Marine Science **74**:1708-1722.

Kerr, L. A., Z. T. Whitener, S. X. Cadrin, M. R. Morse, D. H. Secor, and W. Golet. 2020. Mixed stock origin of Atlantic bluefin tuna in the U.S. rod and reel fishery (Gulf of Maine) and implications for fisheries management. Fisheries Research **224**:105461.

Kulathinal, R. J., L. S. Stevison, and M. A. Noor. 2009. The genomics of speciation in Drosophila: diversity, divergence, and introgression estimated using low-coverage genome sequencing. PLoS genetics **5**:e1000550.

Le Moan, A., D. Bekkevold, and J. Hemmer-Hansen. 2021. Evolution at two time-frames: ancient structural variants involved in post-glacial of the European plaice (*Pleuronectes platessa*). Heredity, 126, 668–683.

Li, H. 2013. Aligning sequence reads, clone sequences and assembly contigs with BWA-MEM. arXiv, 1303.3997 [q-Bio].

Li, H., B. Handsaker, A. Wysoker, T. Fennell, J. Ruan, N. Homer, G. Marth, G. Abecasis, R. Durbin, and G. P. D. P. Subgroup. 2009. The Sequence Alignment/Map format and SAMtools. Bioinformatics **25**:2078-2079.

Lischer, H. E. L., and L. Excoffier. 2011. PGDSpider: an automated data conversion tool for connecting population genetics and genomics programs. Bioinformatics **28**:298-299.

Lowe, W. H., and F. W. Allendorf. 2010. What can genetics tell us about population connectivity? Molecular Ecology **19**:3038-3051.

Luu, K., E. Bazin, and M. G. B. Blum. 2017. pcadapt: an R package to perform genome scans for selection based on principal component analysis. Molecular Ecology Resources **17**:67-77.

Mamoozadeh, N. R., J. E. Graves, and J. R. McDowell. 2020. Genome-wide SNPs resolve spatiotemporal patterns of connectivity within striped marlin (Kajikia audax), a broadly distributed and highly migratory pelagic species. Evolutionary Applications **13**:677-698.

Mariani, S., and D. Bekkevold. 2014. Chapter Fourteen - The Nuclear Genome: Neutral and Adaptive Markers in Fisheries Science. Pages 297-327 *in* S. X.

Mather, F. J., J. M. Mason, and A. C. Jones. 1995. Historical document : life history and fisheries of Atlantic bluefin tuna (p. 165). NOAA Technical Memorandum, NMFS-SEFSC.

McPherson, G. 1991. Reproductive biology of yellowfin tuna in the eastern Australian Fishing Zone, with special reference to the north-western Coral Sea. Marine and Freshwater Research **42**:465-477.

Mérot, C., E. L. Berdan, H. Cayuela, H. Djambazian, A.-L. Ferchaud, M. Laporte, E. Normandeau, J. Ragoussis, M. Wellenreuther, and L. Bernatchez. 2021. Locally Adaptive Inversions Modulate Genetic Variation at Different Geographic Scales in a Seaweed Fly. Molecular Biology and Evolution **38**:3953-3971.

Muhling, B. A., S.-K. Lee, J. T. Lamkin, and Y. Liu. 2011. Predicting the effects of climate change on bluefin tuna (Thunnus thynnus) spawning habitat in the Gulf of Mexico. ICES Journal of Marine Science **68**:1051-1062.

Nikolic, N., F. Devloo-Delva, D. Bailleul, E. Noskova, C. Rougeux, C. Delord, P. Borsa, C. Liautard-Haag, M. Hassan, A. D. Marie, P. Feutry, P. Grewe, C. Davies, J. Farley, D. Fernando, S. Biton-Porsmoguer, F. Poisson, D. Parker, A. Leone, J. Aulich, M. Lansdell, F. Marsac, and S. Arnaud-Haond. 2023. Stepping up to genome scan allows stock differentiation in the worldwide distributed blue shark Prionace glauca. Molecular Ecology **32**:1000-1019.

Nøttestad, L., E. Boge, and K. Ferter. 2020. The comeback of Atlantic bluefin tuna (Thunnus thynnus) to Norwegian waters. Fisheries Research **231**:105689.

Oosting, T., B. Star, J. H. Barrett, M. Wellenreuther, P. A. Ritchie, and N. J. Rawlence. 2019. Unlocking the potential of ancient fish DNA in the genomic era. Evolutionary Applications **12**:1513-1522.

Ovenden, J. R., O. Berry, D. J. Welch, R. C. Buckworth, and C. M. Dichmont. 2015. Ocean's eleven: a critical evaluation of the role of population, evolutionary and molecular genetics in the management of wild fisheries. Fish and Fisheries **16**:125-159.

Patterson, N. J., P. Moorjani, Y. Luo, S. Mallick, N. Rohland, Y. Zhan, T. Genschoreck, T. Webster, and D. Reich. 2012. Ancient admixture in human history. Genetics:genetics. 112.145037.

Pickrell, J. K., and J. K. Pritchard. 2012. Inference of Population Splits and Mixtures from Genome-Wide Allele Frequency Data. PLOS Genetics **8**:e1002967.

Porch, C. E., S. Bonhommeau, G. A. Diaz, A. Haritz, and G. Melvin. 2019. The journey from overfishing to sustainability for Atlantic bluefin tuna, Thunnus thynnus. In B. Block (Ed.). The future of bluefin tunas: Ecology, fisheries management, and conservation (pp. 3-44) John Hopkins University Press.

Portik, D. M., A. D. Leaché, D. Rivera, M. F. Barej, M. Burger, M. Hirschfeld, M.-O. Rödel, D. C. Blackburn, and M. K. Fujita. 2017. Evaluating mechanisms of diversification in a Guineo-Congolian tropical forest frog using demographic model selection. Molecular Ecology **26**:5245-5263.

Puncher, G. N., A. Cariani, G. E. Maes, J. Van Houdt, K. Herten, R. Cannas, N. Rodriguez-Ezpeleta, A. Albaina, A. Estonba, M. Lutcavage, A. Hanke, J. Rooker, J. S. Franks, J. M. Quattro, G. Basilone, I. Fraile, U. Laconcha, N. Goñi, A. Kimoto, D. Macías, F. Alemany, S. Deguara, S. W. Zgozi, F. Garibaldi, I. K. Oray, F. S. Karakulak, N. Abid, M. N. Santos, P. Addis, H. Arrizabalaga, and F. Tinti. 2018. Spatial dynamics and mixing of bluefin tuna in the Atlantic Ocean and Mediterranean Sea revealed using next-generation sequencing. Molecular Ecology Resources **18**:620-638.

Puncher, G. N., A. Hanke, D. Busawon, E. V. A. Sylvester, W. Golet, L. C. Hamilton, and S. A. Pavey. 2022. Individual assignment of Atlantic bluefin tuna in the northwestern Atlantic Ocean using single nucleotide polymorphisms reveals an increasing proportion of migrants

from the eastern Atlantic Ocean. Canadian Journal of Fisheries and Aquatic Sciences **79**:111-123.

Puncher, G. N., S. Rowe, G. A. Rose, N. M. Leblanc, G. J. Parent, Y. Wang, and S. A. Pavey. 2019. Chromosomal inversions in the Atlantic cod genome: Implications for management of Canada's Northern cod stock. Fisheries Research **216**:29-40.

Purcell, S., B. Neale, K. Todd-Brown, L. Thomas, M. A. Ferreira, D. Bender, J. Maller, P. Sklar, P. I. de Bakker, M. J. Daly, and P. C. Sham. 2007. PLINK: a tool set for whole-genome association and population-based linkage analyses. Am J Hum Genet **81**:559-575.

Ravier, C., and J.-M. Fromentin. 2004. Are the long-term fluctuations in Atlantic bluefin tuna (Thunnus thynnus) population related to environmental changes? Fisheries Oceanography **13**:145-160.

Raymond, M. 1995. GENEPOP (version 1.2): population genetics software for exact tests and ecumenicism. The Journal of Heredity. **86**:248-249.

Reiss, H., G. Hoarau, M. Dickey-Collas, and W. J. Wolff. 2009. Genetic population structure of marine fish: mismatch between biological and fisheries management units. Fish and Fisheries **10**:361-395.

Richardson, D. E., K. E. Marancik, J. R. Guyon, M. E. Lutcavage, B. Galuardi, C. H. Lam, H. J. Walsh, S. Wildes, D. A. Yates, and J. A. Hare. 2016a. Discovery of a spawning ground reveals diverse migration strategies in Atlantic bluefin tuna (Thunnus thynnus). Proceedings of the National Academy of Sciences **113**:3299-3304.

Richardson, D. E., K. E. Marancik, J. R. Guyon, M. E. Lutcavage, B. Galuardi, C. H. Lam, H. J. Walsh, S. Wildes, D. A. Yates, and J. A. Hare. 2016b. Reply to Safina and Walter et al.: Multiple lines of evidence for size-structured spawning migrations in western Atlantic bluefin tuna. Proceedings of the National Academy of Sciences **113**:E4262-E4263.

Roberts, D. G., C. A. Gray, R. J. West, and D. J. Ayre. 2010. Marine genetic swamping: hybrids replace an obligately estuarine fish. Molecular Ecology **19**:508-520.

Rochette, N. C., A. G. Rivera-Colón, and J. M. Catchen. 2019. Stacks 2: Analytical methods for paired-end sequencing improve RADseq-based population genomics. Molecular Ecology **28**:4737-4754.

Rodríguez-Ezpeleta, N., N. Díaz-Arce, J. F. Walter III, D. E. Richardson, J. R. Rooker, L. Nøttestad, A. R. Hanke, J. S. Franks, S. Deguara, M. V. Lauretta, P. Addis, J. L. Varela, I. Fraile, N. Goñi, N. Abid, F. Alemany, I. K. Oray, J. M. Quattro, F. N. Sow, T. Itoh, F. S. Karakulak, P. J. Pascual-Alayón, M. N. Santos, Y. Tsukahara, M. Lutcavage, J.-M. Fromentin, and H. Arrizabalaga. 2019. Determining natal origin for improved management of Atlantic bluefin tuna. Frontiers in Ecology and the Environment **17**:439-444.

Rooker, J. R., H. Arrizabalaga, I. Fraile, D. H. Secor, D. L. Dettman, N. Abid, P. Addis, S. Deguara, F. S. Karakulak, A. Kimoto, O. Sakai, D. Macías, and M. N. Santos. 2014. Crossing the line: migratory and homing behaviors of Atlantic bluefin tuna. Marine Ecology Progress Series **504**:265-276.

Rooker, J. R., I. Fraile, H. Liu, N. Abid, M. A. Dance, T. Itoh, A. Kimoto, Y. Tsukahara, E. Rodriguez-Marin, and H. Arrizabalaga. 2019. Wide-ranging temporal variation in transoceanic movement and population mixing of bluefin tuna in the North Atlantic Ocean. Frontiers in Marine Science **6**:398.

Rooker, J. R., D. H. Secor, G. DeMetrio, A. J. Kaufman, A. B. Ríos, and V. Ticina. 2008. Evidence of trans-Atlantic movement and natal homing of bluefin tuna from stable isotopes in otoliths. Marine Ecology Progress Series **368**:231-239.

Rypina, I. I., K. Chen, C. M. Hernández, L. J. Pratt, and J. K. Llopiz. 2019. Investigating the suitability of the Slope Sea for Atlantic bluefin tuna spawning using a high-resolution ocean circulation model. ICES Journal of Marine Science **76**:1666-1677.

Safina, C. 2016. Data do not support new claims about bluefin tuna spawning or abundance. Proceedings of the National Academy of Sciences **113**:E4261-E4261.

Schaefer, K. 1996. Spawning time, frequency, and batch fecundity of yellowfin tuna, Thunnus albacares, near Clipperton Atoll in the eastern Pacific ocien. Fish. Bull. **94**:98-112.

Secor, D. H., J. R. Rooker, B. I. Gahagan, M. R. Siskey, and R. W. Wingate. 2015. Depressed resilience of bluefin tuna in the western atlantic and age truncation. Conservation Biology **29**:400-408.

Siskey, M. R., M. J. Wilberg, R. J. Allman, B. K. Barnett, and D. H. Secor. 2016. Forty years of fishing: changes in age structure and stock mixing in northwestern Atlantic bluefin tuna (Thunnus thynnus) associated with size-selective and long-term exploitation. ICES Journal of Marine Science **73**:2518-2528.

Stephenson, R. L. 1999. Stock complexity in fisheries management: a perspective of emerging issues related to population sub-units. Fisheries Research **43**:247-249.

Suda, A., I. Nishiki, Y. Iwasaki, A. Matsuura, T. Akita, N. Suzuki, and A. Fujiwara. 2019. Improvement of the Pacific bluefin tuna (Thunnus orientalis) reference genome and development of male-specific DNA markers. Scientific Reports **9**:14450.

Thorstensen, M. J., P. T. Euclide, J. D. Jeffrey, Y. Shi, J. R. Treberg, D. A. Watkinson, E. C. Enders, W. A. Larson, Y. Kobayashi, and K. M. Jeffries. 2022. A chromosomal inversion may facilitate adaptation despite periodic gene flow in a freshwater fish. Ecology and Evolution **12**:e8898.

Tigano, A., and V. L. Friesen. 2016. Genomics of local adaptation with gene flow. Molecular Ecology **25**:2144-2164.

Valenzuela-Quiñonez, F. 2016. How fisheries management can benefit from genomics? Briefings in Functional Genomics **15**:352-357.

Viñas, J., A. Gordoa, R. Fernández-Cebrián, C. Pla, Ü. Vahdet, and R. M. Araguas. 2011. Facts and uncertainties about the genetic population structure of Atlantic bluefin tuna (Thunnus thynnus) in the Mediterranean. Implications for fishery management. Reviews in Fish Biology and Fisheries **21**:527-541.

Walter, J. F., C. E. Porch, M. V. Lauretta, S. L. Cass-Calay, and C. A. Brown. 2016. Implications of alternative spawning for bluefin tuna remain unclear. Proceedings of the National Academy of Sciences **113**:E4259-E4260.

Waples, R. 1998. Separating the wheat from the chaff: patterns of genetic differentiation in high gene flow species. Journal of Heredity **89**:438-450.

Waples, R. S. 2022. What Is Ne, Anyway? Journal of Heredity **113**:371-379.

Ward, R. D., Zemlak, T. S., Innes, B. H., Last, P. R., & Hebert, P. D. 2005. DNA barcoding Australia's fish species. Philosophical Transactions of the Royal Society of London. Series B, Biological Sciences, 360(1462), 1847–1857. https:// doi. org/ 10. 1098/ rstb. 2005. 1716

Wellenreuther, M., and L. Bernatchez. 2018. Eco-Evolutionary Genomics of Chromosomal Inversions. Trends in Ecology & Evolution **33**:427-440.

Xuereb, A., C. C. D'Aloia, M. Andrello, L. Bernatchez, and M.-J. Fortin. 2021. Incorporating putatively neutral and adaptive genomic data into marine conservation planning. Conservation Biology **35**:909-920.

Yang, J., S. H. Lee, M. E. Goddard, and P. M. Visscher. 2011. GCTA: A Tool for Genome-wide Complex Trait Analysis. The American Journal of Human Genetics **88**:76-82.

Figure legends

Figure 1. Population structure and connectivity of Atlantic bluefin tuna. (a) Map showing capture location and life stage of Atlantic bluefin tuna samples included in this study. Capture location of adults from the Gulf of Mexico are enclosed within the purple rounded polygon to fulfil confidentiality requirements. (b) Estimated individual ancestry proportions assuming two ancestral populations. (c) Principal Component Analysis (PCA) of genetic variability among Atlantic bluefin tuna samples, following colour codes identical to (b). (d) Density distribution of individual MED-like ancestry proportions per spawning ground. (e) F3 statistics for each combination of sources and target populations, where the Slope Sea and Mediterranean Sea contain larvae and young of the year and larvae, young of the year and adults, respectively (see detailed results in Table S4 and Figure S5). (f) Visual representation of the best-fit demographic model, where arrow and branch widths are proportional to directional migration rates (m) and effective population sizes (n) respectively, and where T represents the duration of population splits. Estimated parameter values are given in units of 2nA, where nA is the effective size of the ancestral population, related to the population-scaled mutation rate parameter of the ancestral populations by $\theta=4nA\mu$.

Figure 2. Outlier markers in Atlantic bluefin tuna cluster within one 2.63 Mb genomic regions showing high long-distance linkage disequilibrium. (a) PCA performed using the 123 outlier SNPs showing the three-cluster grouping (shades of blue) where shapes and colors of samples are those indicated in Figure 1. (b) SNP pairwise linkage disequilibrium plot among the 110 SNPs found within a high linkage region covering scaffolds BKCK01000075 (partially) and BKCK01000111 of the reference genome where most of the SNPs contributing to PC1 from (a) are located. (c) Boxplot showing heterozygosity values (y axis) at the three sample groups shown in (a), represented by the same blue colour code, and based on the 110 SNPs within the genomic region shown in (b). (d) Proportion of samples from each location and age class assigned to each of the three groups shown in (c).

Figure 3. Interspecific introgression between albacore and Atlantic bluefin tuna. (a) Phylogenetic tree estimated by TreeMix based on nuclear data allowing one migration event (the arrow indicates migration direction and rate). Numbers indicate the percentage of individuals (from those included in the tree) showing the introgressed mitochondrial haplotype based on three diagnostic positions retrieved in the 'mito' catalog for each location and age class (abbreviations as in Figure 1). On the upper right, zoom on the phylogenetic relationships among Atlantic bluefin tuna groups. (b) D statistical values estimated from the ABBA/BABA test used to detect introgression from albacore to different targets (rows) using different references (colors). The conceptual trees show the model topology of BABA (left) and ABBA (right) genetic variants. In absence of introgression D-statistic should equal 0, while the higher the value, the more introgressed is the target group respect to the reference and vice versa.

Figure 4. Evolutionary origin of Atlantic bluefin tuna variation within the region of high linkage disequilibrium. (a) Principal component analysis (PCA) including other *Thunnus* species) performed using 156 genetic variants located within the genomic region under high linkage disequilibrium, hosting a candidate structural variant. Albacore tuna (*T. alalunga*) is represented in blue, Southern bluefin tuna (*T. maccoyii*) in green and Pacific bluefin tuna (*T. orientalis*) in yellow, (b) Estimated D values from an ABBA/BABA test based on variants located within the

genomic region of high linkage disequilibrium, using Southern bluefin tuna as an out-group, albacore as a donor species and all different groups of Atlantic bluefin tuna considering spawning area (Mediterranean Sea = MED, Gulf of Mexico = GOM and Slope Sea = SS) and age class (larvae = L, young of the year = Y and adult = A) as alternative targets ordered along the y-axis.

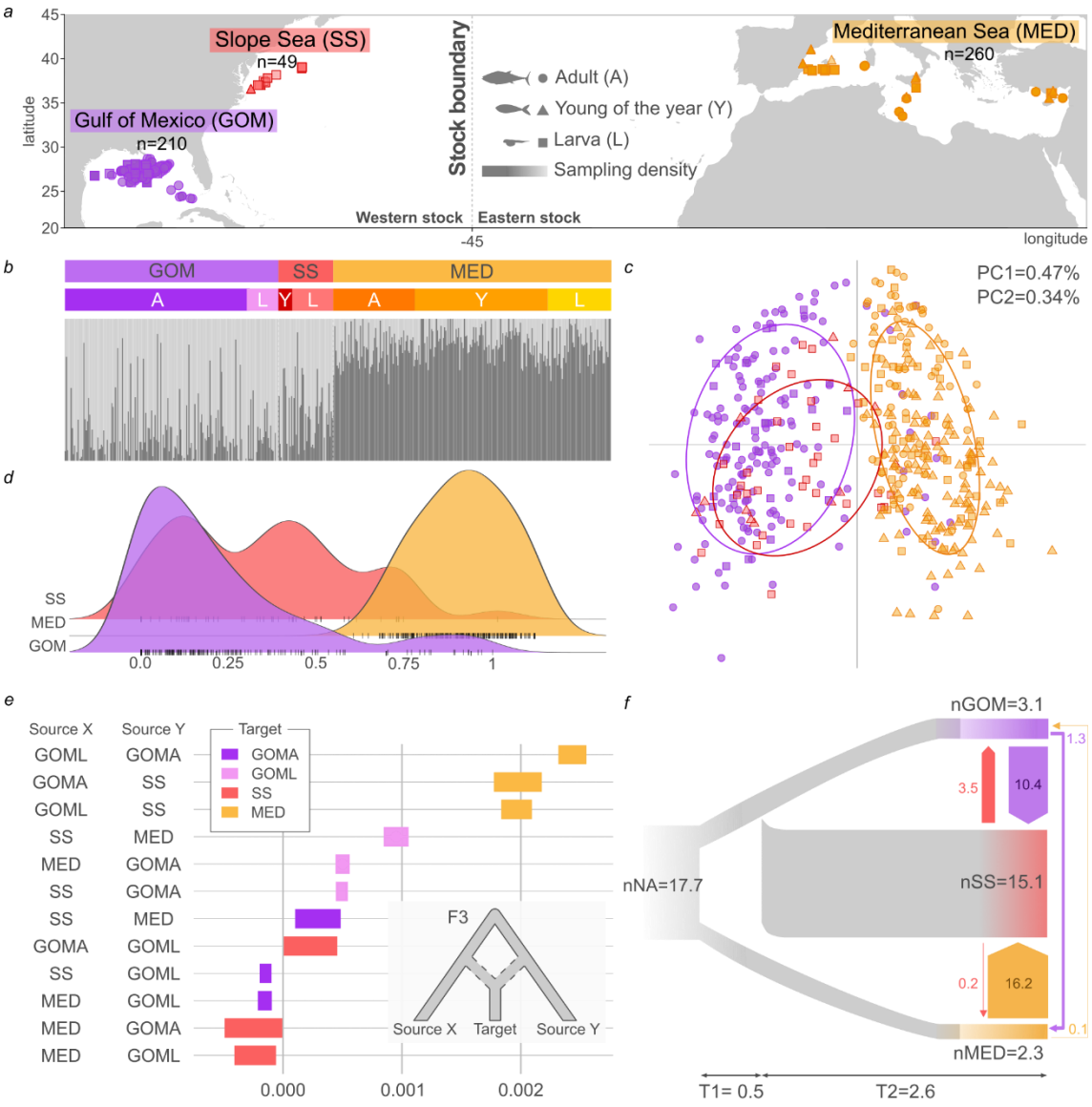

Figure 1. Population structure and connectivity of Atlantic bluefin tuna. (A) Map showing capture location and life stage of Atlantic bluefin tuna samples included in this study. (B) Estimated individual ancestry proportions assuming two ancestral populations. (C) Principal Component Analysis (PCA) of genetic variability among Atlantic bluefin tuna samples. (D) Density distribution of the individual ancestry proportion per spawning ground. (E) F3-statistics for each combination of sources and target combinations where values related to Slope Sea and Mediterranean Sea represent the range of values for Slope Sea larvae and young of the year and for Mediterranean larvae, young of the year and adults (see detailed results in Table S4 and Figure S5). (F) Visual representation of the best fit demographic model, where arrow and branch widths are proportional to directional migration rates (m) and effective population sizes (n) respectively, and where T represents relative time between population splits and Θ, the theta parameter for the ancestral population before the split ($\theta = 4N_A\mu$, with N_A being the effective size of the ancestral population, and μ the per-site mutation rate per generation) to which the rest of estimated parameters are scaled to.

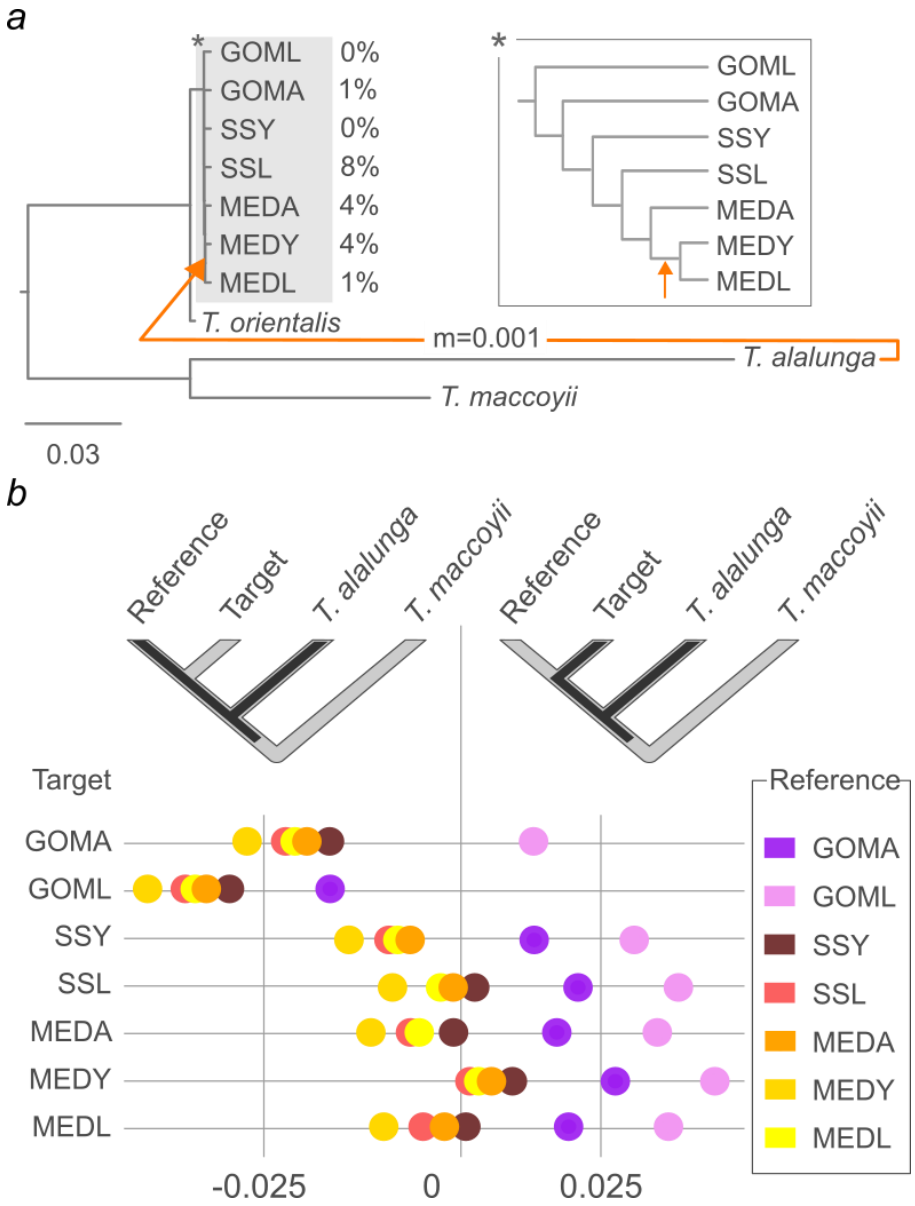

Figure 2. Inter specific introgression between albacore and Atlantic bluefin tuna. (A) Phylogenetic tree estimated by TreeMix based on nuclear data allowing one migration event (the arrow indicates migration direction and rate). Numbers indicate percentage of individuals (from those included in the tree) showing the introgressed mitochondrial haplotype for each location and age class (abbreviations as in Figure 1). (B) D statistical values estimated from the ABBA/BABA test used to detect introgression from albacore to different targets (rows) using different references (colours). The higher the value, the more introgressed is the target group respect to the reference.

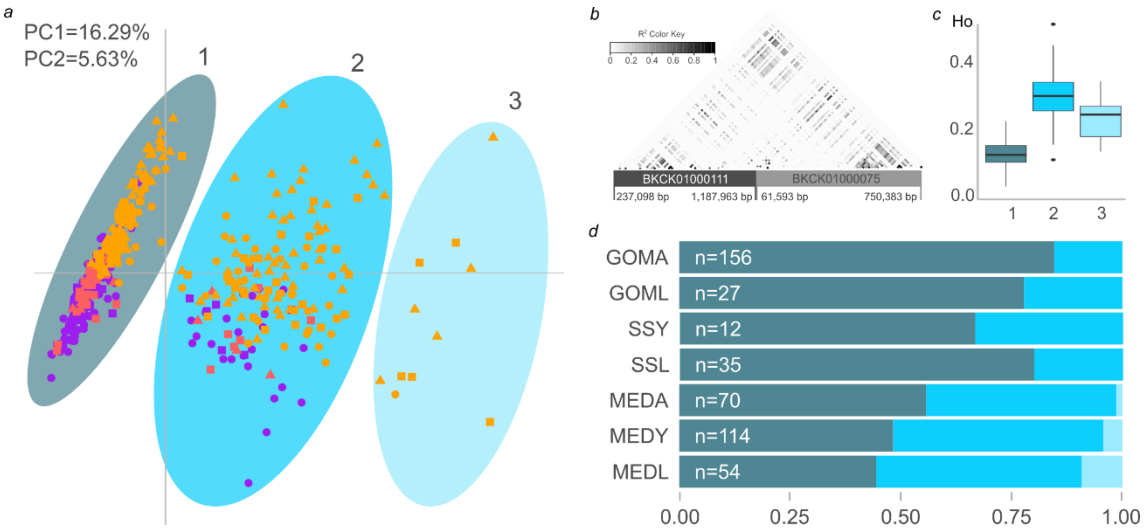

Figure 3. Outlier markers reveal genomic regions under high linkage disequilibrium in Atlantic bluefin tuna. (A) PCA performed using the 123 outlier SNPs showing the three-cluster grouping (shades of blue) where shapes and colours of samples are those indicated in Figure 1. (B) SNP pairwise linkage disequilibrium plot among the 110 SNPs found within the highly linked region covering scaffolds BKCK01000075 (partially) and BKCK01000111 of the reference genome where most contributing SNPs for the PC1 from (A) are located. (C) Boxplot showing heterozygosity values (y axis) at the three sample groups shown in (A), represented by the same blue colour system, and based on the 110 SNPs within the genomic region shown in (B). (D) Proportion of samples from each location and age class assigned to each of the three groups shown in (C).

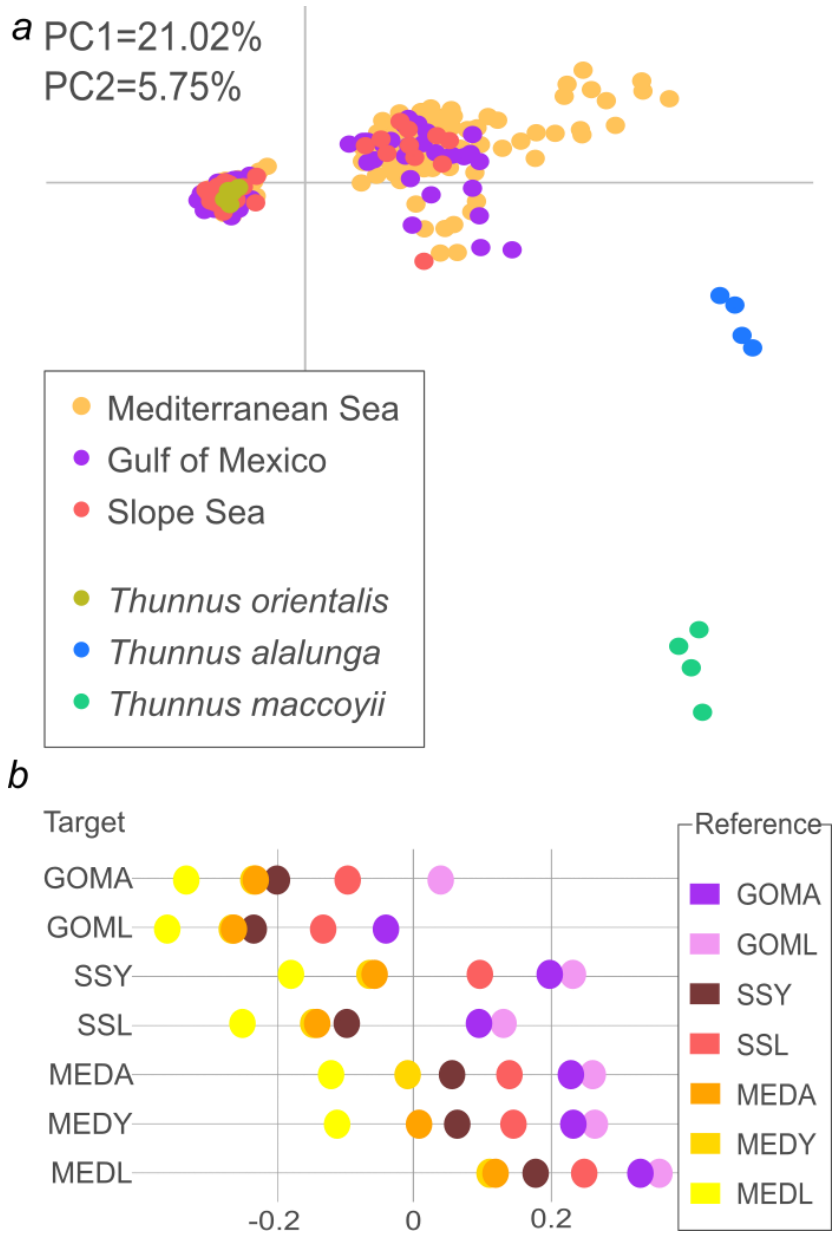

Figure 4. Evolutionary origin of Atlantic bluefin tuna outlier markers within the region under high-linkage disequilibrium. (A) Principal c omponent a nalysis (PCA) including other *Thunnus* species (albacore in blue, Southern b luefin tuna in green and Pacific b luefin tuna in yellow) performed using 156 genetic variants located within the genomic region under high linkage disequilibrium hosting the potential chromosomal inversion. (B) D statistic values estimated performing the ABBA/BABA test based on variants from the genomic region under high-linkage disequilibrium, using Southern b luefin tuna as outgroup, albacore as donor species and all different groups of Atlantic bluefin tuna as target ordered along the y axis.